

DEVELOPMENT OF A FIELD PERMEABILITY TEST FOR ASSESSING THE  
DURABILITY OF CONCRETE IN MARINE STRUCTURES

By

CONSTANTINOS A. MELETIOU

A DISSERTATION PRESENTED TO THE GRADUATE SCHOOL  
OF THE UNIVERSITY OF FLORIDA IN PARTIAL FULFILLMENT  
OF THE REQUIREMENTS FOR THE DEGREE OF  
DOCTOR OF PHILOSOPHY

UNIVERSITY OF FLORIDA

1991

Copyright 1991

by

Constantinos A. Meletiou

TO

MARIA

#### ACKNOWLEDGMENTS

The author gratefully appreciates Dr. Mang Tia, his supervisory committee chairman, for his academic advice, constant encouragement, and dedicated support that made this study possible. His challenging inquiries have always stimulated my academic curiosity. My deep appreciation is due to Dr. David Bloomquist, my supervisory cochairman, for his valuable guidance, expert advice, and contribution to the development of instrumentation. Sincere appreciation goes to Dr. Paul Thompson and Dr. Mark Yang for serving on my supervisory committee and to Dr. Kirk Hatfield for his valuable contribution. I am forever indebted to Dr. Byron Ruth for his contribution to my academic development and exposure to applied concrete engineering.

I would like to extend my gratitude to the Florida Department of Transportation and Federal Highway Administration for providing the financial support for this study. The cooperation of Dr. Jamshid Armaghani, the technical coordinator for this study, Mr. Rodney Powers, and Mr. Ivan Lasa is duly acknowledged. I thank Messrs. Ed Dobson, Danny Richardson, and Patrick Upshaw for their technical support, and Mrs. Irene Scarso for her professional typing and correction of this manuscript.

I am ever grateful to my parents for their love, continuous encouragement and support. As to my companion Ms. Maria Zifou, without whose presence and patience this dissertation would not have been materialized, I express my gratitude. I thank her for being the source of inspiration, encouragement and support during the entire course of my studies, and the catalyst for my intellectual advancement.

## TABLE OF CONTENTS

	Page
ACKNOWLEDGMENTS . . . . .	iv
LIST OF TABLES . . . . .	viii
LIST OF FIGURES . . . . .	ix
ABSTRACT . . . . .	xii
CHAPTER	
1 INTRODUCTION . . . . .	1
1.1 Background and Problem Statement . . . . .	1
1.2 Research Needs . . . . .	3
1.3 Scope and Objectives of the Study . . . . .	4
2 LITERATURE REVIEW . . . . .	6
2.1 Introduction . . . . .	6
2.2 Concrete in Marine Environment . . . . .	6
2.3 Problem of Durability of Marine Concrete Structures in Florida . . . . .	9
2.4 Existing Permeability Tests . . . . .	12
3 DEVELOPMENT OF A FIELD PERMEABILITY TEST METHOD . . . . .	19
3.1 Fundamental Concepts Used in the Design of the FPT . . . . .	19
3.2 Design Considerations and Desirable Features . . . . .	21
3.3 Development of the Prototype . . . . .	22
3.3.1 Design Concept . . . . .	22
3.3.2 Improved FPT Probe . . . . .	22
3.3.3 FPT Instrumentation Unit . . . . .	28

3.4	Development of Analytical Solution . . . . .	31
3.4.1	The Flow Pattern in the FPT . . . . .	31
3.4.2	Derivation of the Packer/Lugeon Equations . . . . .	32
3.5	Investigation on the Effects of Porosity on Permeability of Concrete . . . . .	39
3.5.1	Porosity and Permeability of Concrete . . . . .	39
3.5.2	Determination of the Porosity of Hardened Concrete . . . . .	41
3.5.3	Permeability vs. Porosity . . . . .	43
3.6	Investigation on the Effective Radius of Flow Region . . . . .	45
3.6.1	Concept of Effective Radius of Flow Region . . . . .	45
3.6.2	Relating Volume of Flow to Volume of Saturated Solid Material . . . . .	47
3.6.3	Estimation of Permeability Based on Effective Radius of Flow Region . . . . .	47
3.7	Test Procedure . . . . .	48
3.8	Method of Analysis of Data . . . . .	49
3.8.1	Data Collection . . . . .	50
3.8.2	Data Reduction and Analysis . . . . .	53
3.8.3	Determination of Apparent Permeability Coefficient . . . . .	54
4	EVALUATION OF THE DEVELOPED FPT APPARATUS AND METHOD . . . . .	57
4.1	Laboratory Experimentation . . . . .	57
4.1.1	Evaluation of the Sealing Mechanism of the FPT Probe . . . . .	57
4.1.2	Evaluation of the FPT Instrumentation Unit . . . . .	57
4.1.3	Performance of the FPT Apparatus Under Long-Term Testing . . . . .	58
4.1.4	Effect of Test Orientation . . . . .	58
4.1.5	Effect of Using a Partially Filled Test Section . . . . .	61
4.1.6	Effect of Initial Condition of Concrete . . . . .	64
4.1.7	Effect of Applied Test Pressure . . . . .	66
4.1.8	Flow Characteristics of FPT Under Long-Term Testing . . . . .	71
4.1.9	Evaluation of Repeatability of the FPT . . . . .	73
4.1.10	Correlation Between FPT and Lab Permeability Test Results . . . . .	77
4.2	Field Experimentation . . . . .	82

4.3	Conclusions on the Development of the FPT . . . . .	86
4.3.1	General . . . . .	86
4.3.2	FPT Method . . . . .	87
4.3.3	Analytical Solution . . . . .	88
4.3.4	Effect of Test Variables . . . . .	88
5	TESTING AND EVALUATION OF IN-SERVICE MARINE STRUCTURES . . . . .	89
5.1	Selected Concrete Bridge Structures . . . . .	89
5.2	Field Testing Program . . . . .	108
5.2.1	Field Operations . . . . .	108
5.2.2	Field Permeability Test Results . . . . .	115
5.3	Laboratory Testing Program . . . . .	124
5.3.1	Modification of the Chloride Permeability Test . . . . .	124
5.3.2	Chloride Permeability Test Results . . . . .	127
5.4	Correlation Between the Results of the Developed FPT Method and the AASHTO T277-83 Method . . . . .	128
5.5	Evaluation of the Tested Site Concrete . . . . .	131
6	RECOMMENDED TESTING AND EVALUATION SCHEME USING THE DEVELOPED FPT METHOD . . . . .	138
6.1	Proposed Testing Scheme . . . . .	138
6.2	Recommended Permeability Ranges for the Developed FPT . . . . .	141
7	CONCLUSIONS AND RECOMMENDATIONS . . . . .	145
7.1	Summary and Conclusions . . . . .	145
7.2	Recommendations . . . . .	149
APPENDIX A	FIELD PERMEABILITY TEST--USER'S MANUAL . . . . .	152
APPENDIX B	APPLICATION OF THE PROPOSED TESTING PROGRAM FOR MARINE STRUCTURES . . . . .	174
REFERENCES	. . . . .	182
BIOGRAPHICAL SKETCH	. . . . .	185

## LIST OF TABLES

TABLES	Page
3.1 Estimation of Permeable Pore Space (Effective Porosity) in a Hardened Concrete Specimen . . . . .	44
4.1 Effect of Test Orientation on Flow Rate in the FPT . . . . .	60
4.2 Volumetric Quantity of Water Required to Fill the Test Section . . . . .	62
4.3 Volume of Water Corresponding to Initial Head Drop in Manometer . . . . .	62
4.4 Effect of Initial Condition of Concrete on Flow Rate in the FPT . . . . .	67
4.5 Coefficient of Permeability Determined at Different Applied Test Pressure . . . . .	69
4.6 Permeability of Concrete Specimens as Determined by the FPT and Lab Methods . . . . .	80
5.1 Summary of Results Obtained from FPTs Performed on In-Service Concrete Bridge Structures . . . . .	116
5.2 Repeatability of FPTs Performed at the Same Test Section . . . . .	121
5.3 Comparison of Results Obtained from FPTs Performed on Structural Elements of Same Type and Concrete Material . .	122
5.4 Results of the Rapid Chloride Permeability Tests . . . . .	129
5.5 Comparison of Results Obtained from the FPT and Rapid Chloride Permeability Test . . . . .	132
6.1 Interpretation of FPT Results . . . . .	143

## LIST OF FIGURES

FIGURES	Pages
3.1 Schematic of the FPT Probe and Set-Up . . . . .	23
3.2 Picture of the Initial-Design FPT Probe . . . . .	25
3.3 Picture Showing the Modified FPT Probe . . . . .	26
3.4 Schematic of the Improved Design of the Modified FPT Probe . . . . .	27
3.5 Picture Showing the Developed Portable FPT Instrumentation Unit . . . . .	29
3.6 Schematic of the Portable Field Permeability Test Unit . . . . .	30
3.7 Modeling of the Geometric Configuration of (a) the Flow Region, and (b) the Test Section of the FPT . . . . .	34
3.8 Standard FPT Data Sheet . . . . .	51
3.9 FPT Measurements from B. B. McCormick Bridge, Jacksonville . . . . .	55
4.1 Typical Flows Obtained from FPTs Performed at Different Test Orientations . . . . .	59
4.2 Typical FPT Flows Indicating the Effect of Initial Condition of Concrete . . . . .	65
4.3 Plot of Coefficient of Permeability Determined by FPTs Performed at Different Applied Test Pressure . . . . .	70
4.4 Plot of FPT Results Obtained from Long-Term Laboratory Testing . . . . .	72
4.5 Typical Plot Indicating the Repeatability of the FPT Method When the Concrete is Dry . . . . .	75
4.6 Typical Plot Indicating the Repeatability of the FPT Method When the Concrete is Partially Saturated . . . . .	76

4.7	Correlation Between the Results of the FPT and the Laboratory Permeability Test . . . . .	78
4.8	Correlation Between the Results of the FPT and Laboratory Permeability Test When Concrete is Saturated . . . . .	81
4.9	Picture Showing the FPT Probe Installed on a Pile Column of a Concrete Bridge . . . . .	84
4.10	Picture Showing the Use of the FPT Instrumentation Unit in an On-Going Test . . . . .	85
5.1	Picture Showing the Substructure of the Seven Mile Bridge . . . . .	91
5.2	Picture Showing the Substructure of Long Key Bridge . . . . .	92
5.3	Picture Showing the Substructure of Bahia Honda Southbound (Right) and Northbound (Left) Bridges . . . . .	92
5.4	Picture Showing the Substructure of Niles Channel Old (Right) and New (Left) Bridges . . . . .	93
5.5	Picture Showing the Substructure of B. B. McCormick Bridge . . . . .	93
5.6	Picture Showing the Substructure of SR-206 Bridge . . . . .	94
5.7	Picture Showing the Substructure of Seabreeze Causeway Bridge . . . . .	94
5.8	Picture Showing the Substructure of the Broward River Bridge . . . . .	95
5.9	Picture Showing the Substructure of Horse Creek Bridge . . . . .	95
5.10	Picture Showing the Substructure of the Old Horse Creek Bridge . . . . .	96
5.11	Picture Showing Concrete Deterioration in a Pile (Broward River Bridge, Jacksonville) . . . . .	99
5.12	Picture Showing Concrete Cracking due to Steel Corrosion in a Previously Repaired (Patched) Pile (Broward River Bridge, Jacksonville) . . . . .	100
5.13	Picture Showing Extensive Vertical Cracking due to Steel Corrosion in a Pile (Broward River Bridge, Jacksonville) . . . . .	101
5.14	Picture Showing Cracking of Concrete and Visible Corrosion Products in a Pile (B. B. McCormick Bridge, Jacksonville) . . . . .	102

5.15	Picture Showing Excessive Vertical Cracking and Spalling of Concrete in a Pile (B. B. McCormick Bridge, Jacksonville) . . . . .	103
5.16	Picture Showing Visible Steel Corrosion and Spalling of Concrete Cover in a Pile Cap (Seven-Mile Bridge, Florida Keys) . . . . .	104
5.17	Picture Showing Excessive Steel Corrosion and Extensive Concrete Spalling in a Pier (Seven-Mile Bridge, Florida Keys) . . . . .	105
5.18	Picture Showing the Preparation of a Test Location . . . . .	109
5.19	Picture Showing the Coring of a Test Hole . . . . .	111
5.20	Picture Showing the Location of Extracted Cored Concrete Sample with Respect to the Test Hole . . . . .	112
5.21	Picture Showing the Measurement of In Situ Moisture Content of Concrete . . . . .	114
5.22	Picture Showing a Field Concrete Core (Right) and a Prepared Specimen (Left) . . . . .	125
5.23	Picture Showing the Modified Applied Voltage Cell . . . . .	125
5.24	Correlation Between Charge Passed and Water Permeability Coefficient . . . . .	133
6.1	Proposed Testing Program for Marine Structures . . . . .	139

Abstract of Dissertation Presented to the Graduate School  
of the University of Florida in Partial Fulfillment of the  
Requirements for the Degree of Doctor of Philosophy

DEVELOPMENT OF A FIELD PERMEABILITY TEST FOR ASSESSING THE  
DURABILITY OF CONCRETE IN MARINE STRUCTURES

By

Constantinos A. Meletiou

May 1991

Chairman: Mang Tia  
Cochairman: David Bloomquist  
Major Department: Civil Engineering

This research study presents the development and evaluation of a field permeability test (FPT) apparatus and method for rapid and convenient determination of in situ water permeability of concrete in marine structures. The developed FPT method makes use of Darcy's law, which relates coefficient of permeability to rate of flow, and a high water pressure to accelerate the flow and reduce the time of test. The apparent coefficient of permeability is computed from the measured rate of flow of water into the concrete by means of the Packer/Lugeon equation, whose derivation is presented in this study. The FPT apparatus is characterized by portability, efficiency of operation and economy.

The FPT apparatus was extensively evaluated by performing the FPTs on numerous bridges throughout Florida and also on concrete blocks in the laboratory. The FPT apparatus and method were shown to produce consistent and reliable test results which corresponded closely to those measured by an existing laboratory permeability set-up with known reliability. A

correlation analysis between the results obtained by the two methods was performed using linear regression. A coefficient of determination ( $r^2$ ) of 0.97 was obtained, indicating that the relation between the two methods is highly significant. A correlation analysis between the results obtained by the standard Rapid Chloride Permeability (AASHTO T277-83) test and FPT methods produced an  $r^2$  of 0.90 indicating that there seems to be a linear relationship between the results of these two tests.

While the initial moisture content of the tested concrete could have a significant effect on the FPT results, consistent results were obtained when the test section was pre-saturated prior to testing.

A relationship between permeability and durability of concrete was demonstrated in this study. The concrete material at the tested bridges which exhibited durability problems also demonstrated high permeability. Recommended ranges of the permeability coefficient as determined by the FPT method were established for the relative ranking of tested concrete. A proposed testing scheme for the assessment of the performance and durability of concrete in marine structures is presented.

## CHAPTER 1 INTRODUCTION

### 1.1 Background and Problem Statement

In recent years, the durability of reinforced concrete has been of growing concern as some younger structures are failing to meet the performance levels generally expected and accepted as commonplace for many of the older concrete structures. Deterioration of concrete structures such as bridges, parking garages, dams and other water-retaining structures, is a serious problem, and billions of dollars are needed to restore existing concrete structures in order to keep them in proper and safe operating condition. The root of this problem lies in the deicing salts (primarily sodium chloride) used in many states during the winter months and/or in exposure to extremely aggressive (highly corrosive sea-water) environments such as those encountered in coastal areas. The construction industry is becoming increasingly aware that strength characterization alone is not enough to insure quality and that greater emphasis must be placed on the achievement of good and durable concrete. Concrete researchers have recognized that concrete strength can only be an indirect measure of durability and that other parameters governing the ease of movement of liquids and gases through the concrete would provide a better assessment of quality.

The increasing attention being given to all aspects of concrete durability has highlighted the importance of the concrete to resist the ingress of deleterious agents from the surrounding environment. The

penetration of concrete by materials in solution depends on its permeability. Therefore, the permeability of concrete plays a very important role in influencing the durability of a concrete structure. First, it controls the rate of flow of water, which can cause disruption to the concrete upon freezing. Secondly, it controls the rate of flow of chemicals, such as chloride ions, which can reduce the pH of the concrete and increase the rate of corrosion of the steel reinforcement in the concrete structure.

The way in which liquids, ions (such as chloride ions), and gases (such as carbon dioxide) can penetrate into concrete has, until the last few years, received relatively little attention. There is even less attention paid to the *in situ* permeability of concrete in existing structures, as opposed to the permeability of laboratory-made concrete specimens. It is necessary to distinguish between tests made in the field and those in the laboratory. *In situ* tests on mass concrete are important and often are an essential requirement in the verification of the design. As with other physical properties, the permeability of mass concrete may be markedly affected by conditions which exist in the field. This "field" permeability may well be more significant than the permeability of the concrete material that is determined in the laboratory under ideal or controlled conditions. Simulation of conditions using small scale specimens in the laboratory is an important method for investigating the permeability of concrete material and the influence of various factors that affect this property. At the same time, lab tests can be misleading unless correlated with field behavior in actual structures. Hence, a knowledge of the *in situ* permeability is desirable.

Regardless of how concrete behaves in the structure, chances are that its response and quality will be different when compared with those of standard laboratory specimens. Therefore, *in situ* testing of structural concrete is a necessity since it is difficult to accurately relate "lab-concrete" to "field-concrete."

### 1.2 Research Needs

The permeability of concrete is generally regarded as a fundamental material property governing the durability of concrete, particularly in structures exposed to marine environment. Low permeability of concrete can improve its resistance to water saturation, sulfate and other chemical attack and, most importantly, chloride-ion penetration. Thus, in assessing the durability of a concrete structure, the permeability of the concrete needs to be determined properly.

There does not currently exist any widely used standard performance specification which addresses permeability requirements for concrete designed for structural elements exposed to marine environment. Although there has been some excellent pioneering work in the field of corrosion, there has been relatively little permeability testing performed on in-service concrete structures, either *in situ* or on samples taken from the site. At present, there does not exist any standard method for the direct determination of the *in situ* permeability of structural concrete.

There is a need to develop a testing device which would allow regular *in situ* permeability measurements, i.e., without the requirement to remove cored specimens from the concrete structure and test them in a laboratory permeability test apparatus. Since durability is a function of permeability, there is a need to develop an effective method in assessing

the performance and durability of concrete in marine structures with respect to permeability. It is imperative to understand the importance of this property as a more reliable indicator of the quality of concrete used in marine structures. A testing program for in situ evaluation of in-service marine structures is required in order to obtain permeability data of the concretes used in Florida. There is also a need for the development of concrete performance specifications which include suitable testing (such as laboratory and field permeability tests) for durability and acceptable permeability limits or ranges as design and quality requirements. It is further necessary to determine any relationship that may exist between the rate of corrosion of reinforcing steel and the permeability of the concrete used in marine structures.

### 1.3 Scope and Objectives of the Study

The scope of this research study was to properly assess the performance and durability of existing in-service marine concrete structures under actual field conditions with respect to permeability. The primary objectives of the research study were the following:

1. To modify and improve the prototype field permeability test (FPT) apparatus and method developed in a preceding phase of this study.
2. To fully test and evaluate the developed FPT apparatus and method, and establish, through laboratory and field experimentation, an effective and efficient testing procedure.
3. To implement the FPT apparatus and method in the testing of existing marine structures in order to determine the in situ permeability of concrete under actual field conditions. This

permeability was eventually used to assess the relative performance and durability of the structures under investigation. Since the newly developed FPT was not a standard method, other standardized tests judged suitable for this study were employed in conjunction with the FPT.

4. To investigate and attempt to establish any correlation that may exist between the results of the rapid chloride permeability tests and the results of the FPTs.
5. To attempt to establish recommended limits of permeability indices as determined by the FPT method for durability assessment of structural concrete.

## CHAPTER 2 LITERATURE REVIEW

### 2.1 Introduction

The objectives of the literature survey were to assemble information concerning the permeability of concrete and to review any existing test methods or techniques which were related to the subject of this research study. Since the subject under investigation is related to the durability of marine structures, a brief review of the subject of concrete in marine environment is presented here with particular emphasis given to the durability problems of marine structures in Florida. It should be noted that a large number of laboratory permeability tests have been devised in the past and there is a considerable amount of literature on laboratory investigations into these various test systems. However, any attempt to draw these together and summarize all the laboratory techniques available for permeability measurements was beyond the scope of this research study. The few laboratory studies described in this chapter are presented only for reference purposes. The main focus of the review was on those methods which were relevant to the *in situ* determination of the permeability of concrete or to tests which were related to the subject of interest.

### 2.2 Concrete in Marine Environment

Concrete has been used for many years in marine construction and has proved to be a durable material, generally requiring relatively little maintenance. However, in order to ensure durability, attention must be

given to the specification of concrete for marine structures with due regard to those factors which may affect its performance in practice. Concrete is a durable material if its quality and performance remain acceptable for the design life of the structure. The durability of concrete in a marine environment is only questionable if it deteriorates to a significant extent within the design life of a concrete structure.

The marine environment, from the concrete engineering point of view, can be divided into three main zones:

1. Submerged zone--The totally immersed zone, where the concrete is continuously under water, and oxygen availability for steel corrosion is limited, but the increased hydrostatic pressure can result in a more rapid penetration of seawater into the concrete.
2. Splash zone--Above high tide level, where continuous built-up of salt spray, wetting-drying and freeze-thaw cycles can occur.
3. Atmospheric zone--The inter-tidal zone above the splash zone, where the concrete is kept in a partially wet state and intermittently exposed to air.

Since the severity and type of durability problems are different for different zones, the properties of a concrete mixture need not be the same for an entire concrete structure exposed in marine environment. However, the permeability of concrete is important in all three zones because it influences all physical and chemical phenomena causing concrete deterioration.

Concrete exposed to marine environment may deteriorate as a result of combined effects of chemical action of seawater constituents such as sulfate salts on cement hydration products, alkali-aggregate expansion when reactive aggregates are present, crystallization pressure of salts within concrete if one face of the structure is subject to wetting and

others to drying conditions, frost action in cold climates, corrosion of embedded steel in reinforced or prestressed members, and physical erosion due to wave action and floating objects. Attack on concrete due to any of these causes tends to increase the permeability. This not only would make the concrete material progressively more susceptible to further action by the same destructive agent but also to other types of attack. Thus a complex network of chemical as well as physical causes of deterioration are found at work when a concrete structure exposed to seawater is in an advanced stage of degradation [1].

Permeability is regarded as a fundamental material property governing the durability of concrete, particularly in structures exposed to marine environment [2]. The experts in the field firmly believe that "the permeability of concrete is indeed the key to overall durability," [3, p.5] and is the most important factor for the long-term performance and durability of marine structures [3]. In fact, low permeability improves concrete's resistance to water saturation, sulfate and other chemical attacks and most importantly, chloride-ion penetration, which is considered to be the major problem related to durability of marine concrete structures.

Mehta [2] reviewed the case histories of several concrete structures which had exhibited deterioration on long-term exposure to seawater. These case histories clearly showed that, although physical and chemical interactions between seawater and constituents of portland cement took place as determined from mineralogical analyses of deteriorated concrete samples, serious deterioration did not occur unless seawater was able to penetrate into the interior of the concrete. The author concluded that "permeability rather than the chemistry of concrete was thus identified as the most important factor in long-term durability" [3, p.2].

More recently, P. K. Mehta [3] reviewed additional case histories as well as studies undertaken by other researchers on concrete deterioration in marine environment. The author points out that under adverse service conditions presented by the typical marine environment, even an impermeable concrete could eventually become permeable and therefore vulnerable to a corrosion-cracking cycle leading to serious structural damage. However, the author characteristically emphasizes that, with reinforced concrete structures exposed to marine environment, structural cracking does not lead to corrosion as long as the remaining concrete is impermeable, and especially if the concrete is fully submerged under water. The author states in his conclusions that harmful chemical reactions between the constituents of hydrated cement paste and seawater can be limited to the surface when well known measures to assure low permeability of concrete are rigorously implemented. To produce concrete with very low permeability and to maintain the impermeability in service, the author strongly recommends that it is essential to carry out all three of the following: (a) proportion a concrete mixture that will almost become impermeable with curing, (b) adopt good concreting practice, (c) take measures to prevent excessive concrete cracking in service [3].

### 2.3 Problem of Durability of Marine Concrete Structures in Florida

The predominant, and most severe, durability problem encountered in marine concrete structures exposed to aggressive environments, such as the ones present in the coastal regions of Florida, is corrosion of the steel reinforcement embedded in concrete. This is caused by the intrusion of chloride ions present in the seawater which can reduce the pH of the concrete and destroy the natural passivity of the reinforcing steel and thus

promote the formation of corrosion products. These products exert large tensile forces which cause cracking and subsequent spalling of the concrete cover which, in turn, can lead to severe structural damage. Regions at or near (within 5 miles) the coast of Florida are classified by the FDOT as extremely aggressive (highly corrosive) environments. This classification is based on the following parameters: concentration of chloride ions greater than 2,000 ppm, sulfates greater than 1,500 ppm, resistivity less than 500 ohm-cm, and pH less than 6.0.

Florida has over 1200 miles of coastline. Approximately 3,000 bridges are situated in these coastal waters which contain chlorides in the order of 17,000 ppm which is typical of most ocean waters. In this environment, the average time to the first signs of corrosion of steel reinforcement in concrete is around twelve years. A record survey of 15 marine substructures in Florida showed the time to corrosion in concrete piling to be between 10 and 15 years with a mean time of 11.5 years. By the age of 20 years, virtually all of our marine bridge substructures will require major repairs of components damaged by corrosion. The majority of the corrosion damage occurs in the splash zone where heavy accumulations of chlorides deposit as a result of the wetting and drying effects of tidal cycling. When a sufficient quantity of chloride penetrates the concrete and contacts the surface of the steel reinforcement, corrosion is initiated. When corrosion develops, the corrosion products occupy a volume 2 to 3 times greater than that of the parent steel. These solid product formations create internal tensile stresses that result in cracking and delamination of the concrete. As the corrosion process further progresses, the structure is compromised necessitating major repairs or premature replacement.

According to FDOT estimates, 15 to 20 percent of some 5,000 bridge structures that have been inspected in the state of Florida have already exhibited serious signs of corrosion and concrete deterioration. The great majority of these bridges are in-service marine structures located along the coastal regions of the state. The substructures of these bridges experience severe durability problems such as scaling, cracking, and spalling of concrete, and disbondment of steel reinforcement. Chloride concentrations as high as 19,000 ppm have been recorded in many cases, and substructure elements such as piers, pile columns, and pier/pile caps have exhibited severe corrosion of reinforcing steel in locations within the splash zone. Most of the marine structures built in Florida have to meet a design life requirement of 50 to 75 years (design life includes both structural and functional utility). However, modern marine structures are exhibiting severe problems of corrosion and deterioration even as early as the fifth year of their service life. The Long Key bridge and the Seven Mile bridge located at the Florida Keys region are dramatic examples of the above mentioned problems. Millions of dollars are needed to maintain or restore these in-service structures in order to keep them in proper and safe operating condition. It is estimated that the annual cost of corrosion-related concrete deterioration in Florida's marine bridge structures is between 30 and 50 million dollars in repairs and reduced service life. This amount is expected to increase dramatically as the mean age of our structures increases and construction, maintenance, and rehabilitation costs rise.

There does not currently exist any widely used standard performance specification which addresses permeability requirements for concrete designed for substructure elements of marine structures. Existing design

guidelines followed in Florida lay down minimum cement contents, maximum water/cement ratios and minimum cover to reinforcing and prestressing steels, but fail to stress what these recommendations are actually aimed at, i.e., producing a high quality concrete with as low a permeability as possible which is sufficiently thick over the reinforcing steel to protect it against marine salts. Although there has been some excellent pioneering work in the field of corrosion, there has been relatively little permeability testing performed on in-service concrete structures, either in situ or on samples taken from the site.

#### 2.4 Existing Permeability Tests

A large number of laboratory permeability tests and surface absorption tests have been devised in the past and there is a considerable amount of literature on laboratory investigations into various test systems [4-12]. However, there does not appear to be any widely used standard procedure or test method for determining the water-permeability of concrete, particularly any test method which is relevant to in situ concrete.

Tyler and Erlin [4] have studied a proposed simple laboratory test method for determining the permeability of concrete based on a modified high-pressure apparatus originally intended for determining air content of hardened concrete which was developed by J. D. Lindsay of the Illinois Department of Highways. McMillan and Lyse [5] have studied the permeability of concrete at the Research Laboratory of Portland Cement Association while Norton and Pletta [6] have studied the permeability of gravel concrete in the Mechanics Department at the University of Wisconsin in hope of determining the relationship between permeability and water/cement

ratio, strength, consistency, absorption, cement/void ratio and grading of aggregate. Ruettgers et al. [7] have studied the permeability of mass concrete with particular reference to Boulder Dam primarily to furnish data for making final decisions on the type of construction and the concrete mixtures to be used. Von der Meulen and Van Dijk [8] developed a simple laboratory permeability-testing apparatus at the South African National Building Research Institute. Powers et al. [9] have also studied the permeability of Portland cement paste, and Murata [10] studied the permeability of concrete specimens by means of the diffusion coefficient method.

The various laboratory apparatuses used by these researchers to measure the permeability of concrete were similar in that all of them measured the flow rate of water under pressure through previously prepared and laboratory cured cylindrical concrete specimens after a steady-state flow condition had been reached, with the exception of the method by Murata [10] in which the areas of the portions penetrated by water were used to measure the depth of penetration for determining the diffusion coefficient. Ludirdja et al. [11] have recently developed a simple laboratory apparatus for measuring the water permeability of 1/2-inch thick disks cut from the center of cylindrical concrete specimens using gravity as the pressure head. However, at present only preliminary results have been presented and the apparatus is currently under further refinement.

Although a number of surface absorption tests have been devised in the past [12], the most well-known test, especially in Europe, is the Initial Surface Absorption Test, commonly known as ISAT [13]. Several years ago, this test was incorporated as a standard method in BS-1881 [14]. The ISAT, which was originally developed by Levitt [15,16] for cast stone

products, can be used to measure the rate at which water applied to the surface of concrete in a special cap is absorbed into the concrete under low head. It should be noted that the objective of this test is to predict the durability of a surface layer of concrete, and gives no information on the interior material. In addition, this test measures the surface absorption, not the actual permeability which is a different material property, and typically the absorption of the outer surface is different from that of the bulk of the concrete. There are some practical difficulties in using the test on site, such as obtaining a good seal between the cap and the concrete surface, and determining the moisture condition of the test surface. When used on samples removed from site the initial moisture condition of concrete can be more accurately controlled, but when used on site it is normal to ensure that a period of at least 48 hours has elapsed since any rain has fallen on the test area. Nevertheless, ISAT measurements have been used in the United Kingdom even for specification compliance on precast, paving, and architectural concrete.

In 1973, the British Building Research Establishment (BRE) recognizing the fact that the ISAT values are highly dependent on the condition of the first few millimeters of surface, developed a technique [17] which could be used to assess the air and water permeability of concrete *in situ*. This test, which is frequently called the "Figg method," enables measurements to be made on concrete just below the surface by means of a simple and portable apparatus. It involves drilling a small hole, typically 6 mm in diameter and 30 mm deep, which is sealed at the surface with a silicone rubber plug to provide an air-tight seal. This plug is pierced by a hypodermic needle connected to a vacuum pump, and pressure in the system is reduced by a given amount. The needle is then locked off, and

the time required for air to permeate through the concrete and increase the pressure in the cavity to a specified value is recorded. This is a measure of the rate at which air can flow through the surrounding concrete into the hole and is taken as the air permeability index of the concrete. A modification of the apparatus makes it possible to measure also the water permeability of concrete by monitoring the rate of fall of water in a capillary after injecting water by means of the hypodermic syringe into the small cavity in the concrete. The moisture content of the concrete has a significant effect on the test results, especially at high water/cement ratios ( $w/c = 0.6$ ). Although some improvements to the Figg method [18] had been made, the scatter in the data is quite high indicating the aggregate effects to be substantial. Additional drawbacks of this method include effective sealing and the determination of the coefficient of permeability due to the fact that the values in the Figg method have a more complex relationship to the true concrete permeability than was originally assumed [18].

An in situ test method was developed by Tanahashi et al. [19] for measuring the permeability of concrete placed in a structure under construction. However, the test apparatus employed in this method is such that the tests can either be performed on previously prepared and cured cylindrical (disks) specimens or on building elements having a limited thickness such as walls and floors.

A test method, termed the rapid chloride permeability test, can be used to rapidly assess the relative permeability of various types of concrete to chloride ions. Although this is not a measure of the water-permeability of concrete, this method is reviewed here since it has become the most widely used test for determining the resistance of concrete to

chloride intrusion and subsequent corrosion of reinforcing steel. This test has been adopted by AASHTO (American Association of State Highway and Transportation Officials) as the Standard Method of Test for Rapid Determination of the Chloride Permeability of Concrete under the AASHTO Designation T277-83. Since this is a standard method, only a brief description of the test method is presented here. A detailed description of the instrumentation and testing procedure can also be found in Reference 20.

The method consists of monitoring the amount of electrical current flowing through a test area of a cylindrical concrete specimen when a potential difference of 60Vdc is maintained across the specimen for a period of 6 hours. In this way, chloride ions are forced to migrate out of a 3.0% NaCl-sodium chloride solution (negative), through the concrete material, and into a 0.3N NaOH-sodium hydroxide solution (positive). The total electric charge (in coulombs) which passes through the concrete specimen during the test period is taken as an index of the relative (high, moderate, low, very low) chloride permeability.

Originally, a test procedure and instrumentation were developed by Whiting [20] at Construction Technology Laboratories, Inc., Skokie, Illinois, for measuring chloride permeability of various types of concrete both in situ and in the laboratory. In the field, the topmost reinforcing mat was used as the positive electrode; whereas the standard laboratory unit uses a specially designed test cell, termed "Applied Voltage Cell," to hold a 3.75 in. diameter, 2-in. thick core test specimen. Both set-ups utilize a 3.0% sodium chloride solution as the permeant. Results of these tests were compared with those obtained using the standard 90-day ponding procedure as specified in AASHTO Designation T259-80: Resistance of

Concrete to Chloride Ion Penetration. For the field technique, a correlation coefficient of 0.92 was calculated for the relationship between charge (in coulombs) transmitted and total chloride concentration after 90 days of ponding. While the correlation was highly significant, the quantitative error estimate (percent standard error) was relatively high, about  $\pm 31\%$  [21]. For the laboratory test, a correlation coefficient of 0.83 and standard error of 39% were established for the same relationship. Because of the relatively high standard errors, the test is best utilized to rank concretes in terms of their relative expected chloride permeability rather than as a means to measure the actual permeability of concrete to chloride ions.

At the present time, implementation of the field device is limited by a lack of background data on the effects of clear concrete cover and ambient temperatures on test results [20,21]. In addition, a series of four in situ tests requires that one lane of traffic be closed continuously for a period of five days [21], and test instrumentation be left operating at the test site overnight [20]. In view of these limitations with the field device, the laboratory standard test method AASHTO T277-83 utilizing the applied voltage cell offers the most reliable alternative to the field testing. Although this is not a true in situ test, since a core must be extracted from the structure, sectioned, and vacuum saturated prior to test, the FHWA (Federal Highway Administration) classifies it as such.

In summary, the major problems which are generally encountered in performing laboratory permeability tests on concrete specimens include (1) the great amount of time required for each test, (2) the possible leakage of water through the apparatus and/or the sides of the specimen,

and (3) the extremely low water flow rate which makes an accurate measurement difficult to obtain. The few studies that have been conducted in the area of in situ determination of water permeability indicated that the test devices and methods used thus far also suffered these drawbacks. Field devices are usually expensive and utilize sensitive and sophisticated instrumentation whose operation is either complex or requires special skills. In addition, tests are usually performed under a certain set of conditions or on cored specimens extracted from the structure. These limitations make such devices unsuitable for testing large structural elements of existing concrete structures under actual field conditions.

## CHAPTER 3 DEVELOPMENT OF A FIELD PERMEABILITY TEST METHOD

### 3.1 Fundamental Concepts Used in the Design of the FPT

The flow of water through concrete is fundamentally similar to flow through any porous medium such as soil, masonry or rock. The analysis of flow through porous materials is a very complex problem. As a result of these complexities, present-day knowledge of the behavior of flow through such materials relies almost entirely on empirical approaches. Literally, thousands of experiments have been performed since Darcy's historical tests were performed in 1856. The variety of empirical relations developed from these tests gives quite conflicting, and often, misleading results. Scheidegger [22] points out that a general relation for flow through porous materials can be developed only if one is able to understand exactly how all these properties (of the porous media) are conditioned by the geometrical properties of the pore system. Such an understanding will be possible when a variety of solutions of the fundamental equations of flow in porous materials have been obtained.

Fluid flow, diffusion, and electrical conduction in porous media take place within extremely complicated microscopic boundaries that make any rigorous solution of the equations of change in the capillary network practically impossible. This is one of the reasons why many researchers in the field of "flow through porous media" have tried, as much as possible, to concentrate on the continuum approach in which no attention is paid to pores or pore structure. The other reason is that continuum

mechanics is often adequate for the phenomenological description of macroscopic transport processes in porous media. At the macroscopic level, the flow can be treated in terms of a few variables that are easily determined in field practice. Hence, in this study the movement of water through porous media was examined from the macroscopic point of view.

The design of a test apparatus for the determination of the in situ water permeability of concrete was based on the concept of drilling a hole from the surface of the concrete, sealing off a section of a hole, and "forcing" water to permeate the concrete mass radially. A similar concept was used by Figg [17] for the determination of the air and water permeability of concrete. After an extensive and thorough review of the available literature pertinent to the subject of this study, it was concluded that a derivative of the borehole tests used in soil or rock engineering could be used to measure the in situ water-permeability of structural concrete. In addition, the analogies which exist between heat-flow, radial flow of pumped wells, and flow of water through concrete provided the basis for the development of an analytical solution to this problem.

Review of Darcy's law showed that the flow,  $Q$ , or the rate of flow,  $q$ , of the water is proportional to the applied pressure,  $P$ , when all other parameters remain constant. Therefore, by increasing the applied pressure, the rate of flow of water through the concrete mass can be increased, thus allowing for faster determination of the coefficient of permeability.

The basic concept involved in the design of a field permeability test apparatus was to drill a hole from the surface of the concrete, seal off the top and bottom of the hole, and apply a high pressure to force the

water to permeate the concrete mass radially. By measuring the rate of flow into the hole the coefficient of permeability could be determined.

### 3.2 Design Considerations and Desirable Features

In the development of a suitable field permeability test apparatus, the following desirable features and design characteristics were considered:

1. The apparatus should be
  - (a) portable,
  - (b) simple and safe to set up and operate,
  - (c) easily and economically reproduced, and
  - (d) inexpensive to operate and maintain.
2. The test method and set-up should be
  - (a) rapid,
  - (b) able to provide accurate and reliable measurements in a short period of time, and
  - (c) as nondestructive as possible (i.e., cause minimum visual and structural damage).

An effective design would be one that incorporates as many of the above desirable features as possible. However, the most important single characteristic that should be considered at the design stage of the test method is the accuracy of the measurements and the reliability of the test results. The development of a test apparatus which satisfies this important requirement will provide a valuable tool for proper evaluation of water permeability of in-service concrete structures under actual field conditions.

### 3.3 Development of the Prototype

#### 3.3.1 Design Concept

In the development of a portable, quasi nondestructive device to measure the *in situ* water permeability of in-service concrete, several different designs were attempted, and a number of devices were constructed and evaluated until the current prototype apparatus was finally adopted. After months of experimentation, an effective design was achieved, and a suitable FPT apparatus, which satisfied all the design requirements set forth in this study, was fabricated. The apparatus relies on the accelerated radial flow of water into the concrete under the influence of an externally applied high pressure. The design concept of the FPT probe and set-up is presented in the schematic diagram shown in Figure 3.1.

#### 3.3.2 Improved FPT Probe

Further refinement and modification was applied to the original FPT probe which was developed in a previous research study [23] in order to improve the sealing mechanism and simplify the dismantling of the test probe. After the completion of a test, the original device was normally dismantled by first releasing the top nut and subsequently removing the top packer from the test hole by applying pressure in the test section high enough to cause it to pop out. The device was then removed by releasing the bottom packer using the special T-socket. The bottom packer could only be reached when the top one was completely taken out and removed from the stem (rod) of the device. Whenever the top packer was damaged, torn, or squeezed into the hole and could not be moved freely, there was no access to the bottom packer, which was still expanded. In such an event, the FPT probe could not be readily dismantled and a pull-out device had to be used in order to remove the FPT probe from the test hole. This

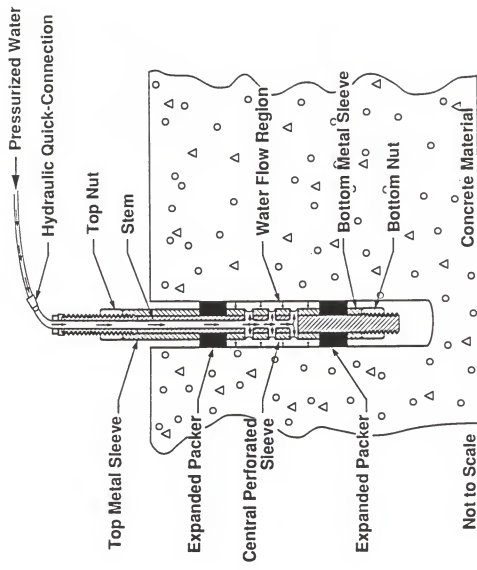


Figure 3.1 Schematic of the FPT Probe and Set-Up

could cause considerable delay in the field operation. In addition, the bottom neoprene packer could be damaged to an extent that it would not be able to be reused in other tests. In order to eliminate this problem, the original FPT probe was modified. Figure 3.2 shows the initial-design FPT probe while Figures 3.3 and 3.4 show the improved probe. In the new design, the interior nuts and all the washers were eliminated. The fine threaded stem was replaced with a smooth rod with fine threads only at its ends where the external nuts were positioned. A perforated metal sleeve, of length equal to the prescribed length of the test section, was placed between the top and bottom packers at the position where the smooth rod is perforated. The assembly was completed by placing a metal sleeve on the exterior side of the neoprene packers at each end of the rod as shown in Figure 3.4. Since the nut at the bottom end of the rod restricts any downward movement, this alternate metal sleeve-packer arrangement works as a single interactive unit. When the top nut is tightened, the neoprene packers are simultaneously compressed against the metal sleeves. In this way the packers are forced to expand at the same rate thus sealing off the section of the hole to be tested. Conversely, by releasing the top nut, both packers are simultaneously released, and the device can readily be removed from the test hole. With this modification, the aforementioned problem was eliminated, the set-up and dismantling of the apparatus was simplified, and the overall design of the FPT probe was improved. Trial tests were performed with two newly fabricated modified FPT probes which were assembled in cylindrical transparent acrylic tubes that allowed observation of the test section. It was concluded that the sealing mechanism of the metal sleeve-packer arrangement had performed properly. Trial tests run on laboratory prepared concrete specimens indicated that the modified FPT probes were operating satisfactorily.

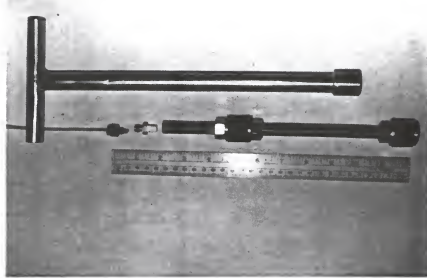


Figure 3.2 Picture of the Initial-Design FPT Probe



Figure 3.3 Picture Showing the Modified FPT Probe

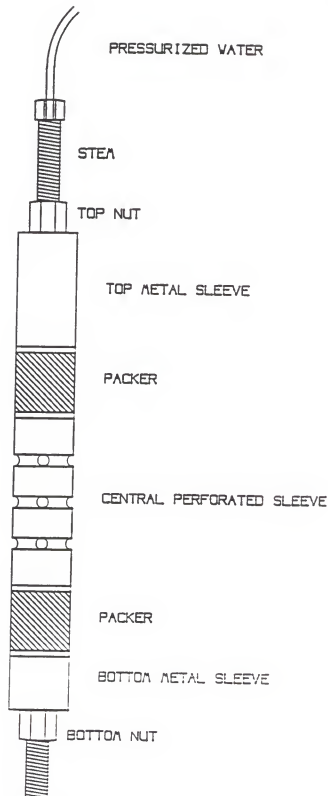


Figure 3.4 Schematic of the Improved Design of the Modified FPT Probe

### 3.3.3 FPT Instrumentation Unit

A portable field permeability test unit with the complete instrumentation required to perform FPTs on concrete has been fabricated. The complete unit is enclosed in a high quality aluminum instrumentation carrying case with a central control panel attached to the lower shell, and a manometer set-up mounted on the upper shell. A picture of the unit is shown in Figure 3.5. The schematic of the unit is shown in Figure 3.6. The following instruments and devices are affixed to the central control panel: (1) a high resolution test pressure gage (max. 1000 psi), (2) a high pressure regulator (max. 6000 psi), (3) two test on/off valves, a pressure relief valve, and a system replenish valve, (4) a 5-way flow valve, and (5) hydraulic quick-connections. High strength (2700 psi) nylon tubing was used in all the connecting lines as well as in the manometer set-up, and teflon tape was applied in all threaded parts of the unit. All the parts of the unit were tested for safety, and the operation of the individual components was checked before the finalized test unit was put together.

In the running of an FPT, the FPT probe is connected to the central control panel through the hydraulic quick-connection. The central control panel provides the quick-connections to allow easy connection of an air pressure source (by means of a portable pressurized nitrogen tank), a vacuum source (by means of a portable hand-operated vacuum pump) and a water source (by means of a portable water tank) to the FPT system. The valve-switch on the central control panel allows for convenient selection of what is to be connected to the FPT probe. The four selections on the valve-switch are (1) pressure release vent, (2) vacuum, (3) water, and (4) manometer (or the test position). For example, if the valve-switch is at

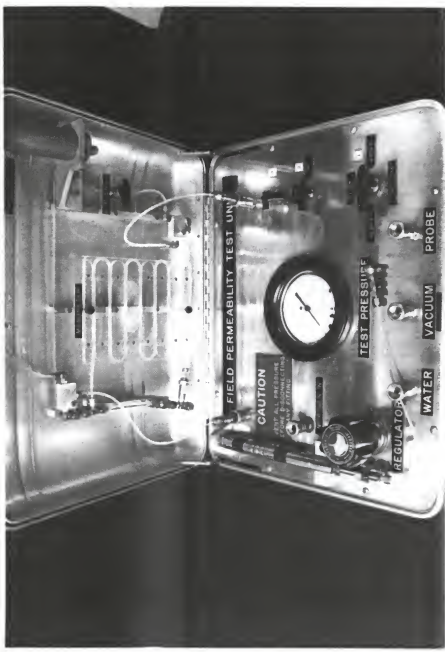


Figure 3.5 Picture Showing the Developed Portable FPT Instrumentation Unit

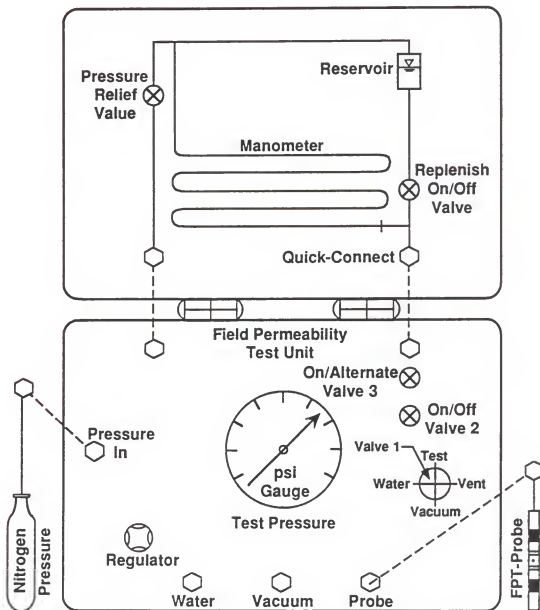


Figure 3.6 Schematic of the Portable Field Permeability Test Unit

the vacuum position, the vacuum source is then channeled to be connected to the FPT probe which in turn is connected to the central control panel through the probe quick-connection. The central control panel also provides for convenient control of the externally applied pressure to the FPT system by means of the pressure gage and regulator. The upper shell of the aluminum carrying case contains the manometer for monitoring the water flow during an FPT and a small high-pressure water-reservoir (100 cc) which provides convenient replenishment of water to the manometer for continuous and uninterrupted test runs. The evaluation of the FPT instrumentation unit is presented in Chapter 4.

### 3.4 Development of Analytical Solution

#### 3.4.1 The Flow Pattern in the FPT

It is interesting to note that Darcy's law is a linear law, similar to Newton's law of viscosity, Ohm's law of electricity, Fourier's law of heat conduction, and Fick's law of diffusion [24]. It is also an essential assumption in the quantitative theory of incompressible flow in aquifers (Laplace equation) as well as other theories and methods of ground-water hydrology, rock and soil mechanics. The well-known Laplace equation similar to the one frequently used for determining the steady flow of a non-compressible homogeneous fluid, such as water, through an isotropic and uniform porous body is normally used to express the steady state flow in rock masses. This equation has been solved by formal mathematical methods for a very large number of cases of plane flow corresponding to various boundary conditions. Values of the coefficient of permeability, as measured by radial flow across rock cores with a central hole, presented in the literature often show wide variations. It is believed that

in most of the cases reported, the permeability of the rock results from open fissures and thin joints and not from the more uniformly distributed pores as in the case of concrete.

Another common situation in which radial flow is encountered is flow toward a pumped well. The mathematical expression for a removal of heat at a constant rate from a homogeneous, infinite slab has provided a useful analogy for study of groundwater flow to a pumping well.

The analogy used between heat and groundwater flow is a classic example of application of knowledge from a branch of science such as physics or mathematics to problems of engineering. Review of studies on constitutive relations for concrete, rock and soils made by a number of researchers [25] further shows the analogies which exist in the flow of water through these porous media. Since the equations used (such as Darcy and Laplace) also govern a number of other physical phenomena, such as flow of heat, free surface flow of water and flow of electricity, the mathematical solutions obtained for those phenomena can be used for the flow of water through concrete. As it is presented later, these strong analogies which exist between the fundamental laws of the various forms of flow and the flow of water through concrete were used as a basis for the development of a test method for the determination of the in situ permeability of concrete.

### 3.4.2 Derivation of the Packer/Lugeon Equations

In order to verify the validity of the Packer/Lugeon equations used in the analysis of the FPT results and data, a mathematical derivation of these equations was sought. After an extensive review of the fundamental principles governing the flow of water through porous media, an analytical solution of the flow problem encountered in the FPT was achieved. The

following mathematical derivation was based on the analysis presented by M.E. Harr [26], and the analogies which exist between the fundamental laws of the various forms of flow and the flow of water through concrete. It should be pointed out that this problem was examined from the macroscopic point of view and was based on the continuum approach in which no attention is paid to the pores or pore structure of the concrete. Figure 3.7 shows how the geometric configuration of the FPT set-up was modeled for this analysis. According to the continuum approach and in order to simplify the problem, the following assumptions were employed in this analysis:

- a) Semi-infinite porous medium
- b) Homogeneous material
- c) Uniform and continuous flow region
- d) Steady-state/spherical flow

The following parameters are defined:

$R$  = Radius of influence (i.e., the effective radius of the flow region under study)

$\phi(R)$  = The potential at a distance  $R$  from the center of the sphere.

The discharge,  $Q$ , at any radial distance  $\rho$  from the source at the center of the sphere (see Figure 3.7 (a)) is

$$Q = 4\pi\rho^2v_\rho = 4\pi\rho^2 \frac{\partial\phi}{\partial\rho} \quad (3.1)$$

$$\frac{\partial\phi}{\partial\rho} = \frac{Q}{4\pi\rho^2}$$

where

$4\pi\rho^2$  = surface area of sphere

$v_\rho$  = radial velocity

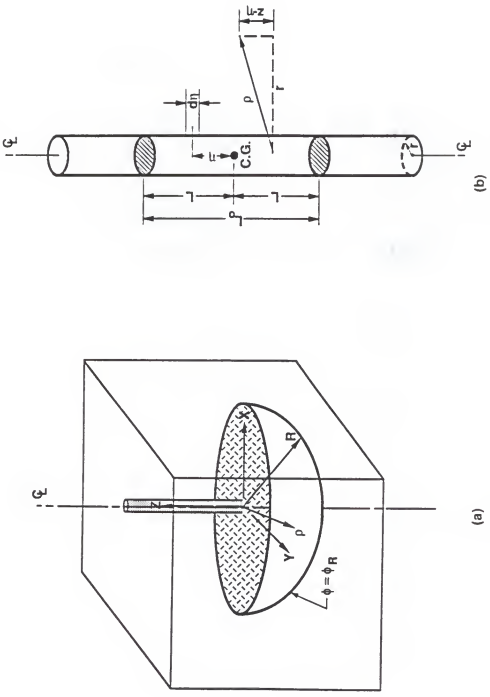


Figure 3.7 Modeling of the Geometric Configuration of (a) the Flow Region, and (b) the Test Section of the FPT

By integrating Eqn (3.1),  $\int d\phi = \int \frac{Q}{4\pi\rho^2} dp$

we get that the potential,  $\phi$ , is

$$\phi = -\frac{Q}{4\pi\rho} + C \quad (3.2)$$

Equation (3.2) indicates that in the case of spherical flow the potential varies inversely with the radius. According to Harr [26], this is a more rapid variation than the simple radial flow problem.

In order to determine the constant of integration "C" in Eqn (3.2), the boundary conditions at the hole should be defined as follows:

$$\rho = r, \text{ and } \phi = \phi_o$$

Therefore, by solving Eqn (3.2) with respect to "C" we get

$$C = \phi_o + \frac{Q}{4\pi r} \quad (3.3)$$

By applying the boundary conditions, and substituting equation (3.3) into (3.2), we get

$$\phi = \frac{Q}{4\pi} \left( \frac{1}{r} - \frac{1}{\rho} \right) + \phi_o \quad (3.4)$$

where  $r \leq \rho \leq R$

Referring to Figure 3.7(b), the following parameters are thus defined:

$2r$  = Diameter of test hole

$L_o = 2L$  = Length of test section

The discharge,  $Q$ , can be assumed to be constant along the test section, and the discharge per unit length can be expressed as

$$\frac{d\varphi}{d\eta} = \frac{\varphi}{2L} \rightarrow d\varphi = \frac{\varphi}{2L} d\eta \quad (3.5)$$

Assuming Eqn. (3.2) to represent the potential at any point in the flow region,

$$d\phi = \frac{d\varphi}{4\pi\rho} \quad (3.6)$$

From the cylindrical coordinate system shown in Figure 3.7(b),

$$\rho = \sqrt{x^2 + (z - \eta)^2} \quad (7)$$

By combining Eqns. (3.5), (3.6) and (3.7), we get

$$\begin{aligned} d\phi &= \left( \frac{\varphi}{2L} \right) d\eta \left( \frac{1}{4\pi\rho} \right) \\ \Rightarrow d\phi &= \left[ \frac{\varphi}{8\pi L \sqrt{x^2 + (z - \eta)^2}} \right] d\eta \end{aligned}$$

Set the limits of integration from  $-\frac{L_o}{2}$  to  $\frac{L_o}{2}$

(note that  $L_o = 2L$ )

$$\phi(x, z) = \frac{\varphi}{8\pi L} \int_{-L}^{+L} \frac{d\eta}{\sqrt{x^2 + (z - \eta)^2}} \quad (3.8)$$

Multiply Eqn. (3.8) by  $\left(\frac{1/x}{1/x}\right)$ :

$$\phi(x, z) = \frac{\varphi}{8\pi L} \int_{-L}^{+L} \frac{(1/x) d\eta}{(1/x) \sqrt{x^2 + (z - \eta)^2}}$$

$$\begin{aligned}
 &= \frac{Q(1/x)}{8\pi L} \int_{-L}^{+L} \frac{d\eta}{\sqrt{\frac{x^2}{x^2} + \frac{(z-\eta)^2}{x^2}}} \\
 &= \frac{Q(1/x)}{8\pi L} \int_{-L}^{+L} \frac{d\eta}{\sqrt{1 + \left(\frac{z-\eta}{x}\right)^2}}
 \end{aligned} \tag{3.8A}$$

By setting  $x = \left(\frac{z-\eta}{r}\right)$ , and taking the derivative of both sides as  $dx = -\frac{d\eta}{r}$ , we get  $d\eta = -r dx$ , which is then substituted into Eqn. (8A) as follows:

$$\begin{aligned}
 \phi(x, z) &= \frac{Q(1/x)}{8\pi L} \int_{\frac{z+L}{r}}^{\frac{z-L}{r}} \frac{-r dx}{\sqrt{1 + x^2}} \\
 &= \frac{-Q}{8\pi L} \int_{\frac{z+L}{r}}^{\frac{z-L}{r}} \frac{dx}{\sqrt{x^2 + 1}}
 \end{aligned} \tag{8B}$$

Recall that  $\sinh^{-1}(x) = \ln(x + \sqrt{x^2 + 1})$  for all  $x$ , and  $\sinh^{-1}(-x) = -\sinh^{-1}(x)$ .

Therefore,

$$\begin{aligned}
 \frac{d\sinh^{-1}(x)}{dx} &= \frac{1 + \frac{2x}{2\sqrt{x^2 + 1}}}{x + \sqrt{x^2 + 1}} \\
 &= \frac{1}{\sqrt{x^2 + 1}}
 \end{aligned}$$

By performing the integration, Eqn. (3.8B) is thus reduced to

$$\phi(x, z) = \frac{-Q}{8\pi L} [\sinh^{-1}(x)] \Big|_{\frac{z+L}{r}}^{\frac{z-L}{r}}$$

$$\begin{aligned}
 &= \frac{-Q}{8\pi L} \left[ \sinh^{-1}\left(\frac{z-L}{r}\right) - \sinh^{-1}\left(\frac{z+L}{r}\right) \right] \\
 \Rightarrow \phi(r, z) &= \frac{Q}{8\pi L} \left[ \sinh^{-1}\left(\frac{z+L}{r}\right) - \sinh^{-1}\left(\frac{z-L}{r}\right) \right] \quad (3.9)
 \end{aligned}$$

According to M. E. Harr [26], the equipotential surfaces given by Eqn. (3.9) are seen to be ellipsoids.

By assuming  $z = 0$  and substituting  $L_o = 2L$ , Eqn. (3.9) becomes

$$\phi(r) = \frac{Q}{2\pi L_o} \sinh^{-1}\left(\frac{L_o}{2r}\right) \approx \frac{Q}{2\pi L_o} \ln\left(\frac{L_o}{r}\right) \quad (3.10)$$

where  $\sinh^{-1}(x) = \ln(x + \sqrt{x^2 + 1})$ , and if  $x \gg 1$ ,  $\sinh^{-1}(x)$  is approximately equal to  $\ln(2x)$ .

Finally, if we substitute in Eqn. (3.10)  $Kh = \phi$ , and solve with respect to the permeability,  $K$ , we obtain

$$K = \frac{Q}{2\pi L_o h} \sinh^{-1}\left(\frac{L_o}{2r}\right); \text{ for } r \leq L_o < 10r \quad (3.10A)$$

$$\text{and } K = \frac{Q}{2\pi L_o h} \ln\left(\frac{L_o}{r}\right); \text{ for } L \geq 10r \quad (3.10B)$$

where  $K$  = coefficient of permeability

$h$  = applied pressure head

Equations 3.10A and 3.10B are usually referred to as the "Packer/Lugeon" equations, and are the ones used by the U.S. Bureau of Reclamation for in situ determination of rock mass permeability. The analysis

presented above constitutes the mathematical derivation of the analytical solution to the flow phenomenon encountered in the FPT.

### 3.5 Investigation on the Effects of Porosity on Permeability of Concrete

#### 3.5.1 Porosity and Permeability of Concrete

The most important macroscopic pore structure parameters which are related to porous materials such as concrete are the porosity, and the permeability. Greenkorn [27] indicates that there may be a correlation between porosity and permeability, but they certainly do not regress. Permeability cannot be predicted from porosity alone since additional parameters which contain more information about pore structure are needed. More specifically for concrete, Neville [28] clearly states that the permeability of concrete is not a simple function of its porosity, but depends on the size, distribution, and continuity of the pores.

Permeability is the term used for the conductivity of a porous medium with respect to permeation by a fluid. The permeability is strictly defined as the property of a porous material which characterizes the ease of fluid flow into or within the material due to combination of pressure, humidity, and temperature differentials, or due to solutions of different concentrations (osmotic effects).

Flow in porous media requires a description of both the media and the flow. A porous medium generally is an extremely complicated network of channels and obstructions. Concrete is a composite material; particles of aggregate are contained in a continuous matrix of mortar which itself comprises a mixture of cement paste and smaller aggregate particles. A porous medium is isotropic with respect to permeability if it is equally permeable to flow in all directions. In the case of concrete, which is

considered to be an isotropic material, the flow of water through its thin pores is viscous and assumed to be laminar, since the permeability is very low and the velocity of percolation is very small. It is normally accepted that the flow of water through concrete follows Darcy's law, although important discrepancies can be found, e.g., when the velocity of percolation is high and the flow is turbulent.

The matrix of a porous medium is the material in which the holes or pores are imbedded. The manner in which the holes are imbedded, how they are interconnected, and the peculiarity of their location, size, shape, and interconnection characterize the porous medium. Permeability is related to the pore size distribution since the distribution of the sizes of entrances, exits, and lengths of the pore walls make up the major resistance to flow. Permeability is the single parameter that reflects the conductance of a given pore structure. Porosity is a quantitative property that describes the fraction of the medium that contains voids. In defining porosity the complex network of voids is replaced with a single number that represents an average property. A porous medium of a given porosity can be extremely different from another porous medium that has the same porosity [28], and it is possible for two porous bodies to have similar porosities but different permeabilities [29].

Porosity macroscopically characterizes the effective pore volume of the medium or, more simply, porosity is the fraction of the bulk volume of the porous sample that is occupied by pore or void space. There are two kinds of pore or void space--one which forms a continuous phase within the porous medium, called "interconnected" or "effective" pore space, and the other which consists of "isolate" or "noninterconnected" pores or voids dispersed over the medium. Noninterconnected voids or pore space cannot

contribute to transport of matter across the porous medium; only the interconnected or effective pore space can. "Dead-end" or "blind" pores are interconnected only from one side. Even though these pores can often be penetrated, they usually contribute only negligibly to permeability. Therefore, only the pores or fraction of the medium that contributes to flow constitutes the "effective porosity."

It is important to differentiate between the permeability and the porosity of a porous material such as concrete. For example, a material could contain a number of small discrete voids such as in a lightweight material but if the voids are not interconnected then the permeability of the material may remain low. On the other hand, if there are a number of connected pores through the material which may even exhibit a high density, the permeability could be high. It is obviously quite possible for two porous media of the same porosity to have entirely different permeability. In fact, only one large passage connecting capillary pores will result in a large permeability, while the porosity will remain virtually unchanged. As Scheidegger [22] characteristically states, a simple consideration of the theoretical possibilities of the structure of porous media makes one realize that a general and simple correlation between porosity and permeability cannot exist.

### 3.5.2 Determination of the Porosity of Hardened Concrete

There does not exist any standard method for determining the effective porosity of hardened concrete. However, ASTM C642 is a standard test method for the determination of specific gravity, percent absorption, and percent voids in hardened concrete. Using this method the total fraction of permeable voids (in percentage) present in a cylindrical concrete

specimen (from batch #35) of 4-inch (10.154 cm) diameter and 1.91 inch (4.853 cm) thickness was determined as follows:

A	= grams of oven-dry sample in air	= 839.80
B	= grams of saturated surface-dry sample in air after immersion	= 884.20
C	= grams of SSD sample in air after immersion and boiling	= 887.10
D	= grams of sample suspended in water after immersion and boiling	= 495.30
g1	= dry bulk specific gravity, A/(C-D)	= 2.14
g2	= apparent specific gravity, A/(A-D)	= 2.44
Absorption after immersion,	[(B-A)/A]*100	= 5.287%
Absorption after immersion and boiling	[(C-A)/A]*100	= 5.632%

PERMEABLE PORE SPACE (VOIDS), %

$$= [(g_2 - g_1) / g_2] * 100 = \underline{12.30 \%}$$

Another concrete specimen (from batch #33), having approximately the same dimensions as the one used in the above experiment, was estimated (using ASTM C642) to have a permeable pore space of 9.93% which corresponded to approximately 373 cc of solids and 38 cc of permeable voids.

It should be noted that this method provides only an estimate of the pore space, and ASTM does not provide a precision statement for this method due to insufficient data available. ASTM indicates that depending on the purposes for which the test results are desired, the procedures of this method may be adequate, or they may be insufficiently rigorous. Caution should be taken in interpreting the results of this ASTM test with respect to permeability since no information on the pore size distribution and the pore entry radii is provided by this method.

ASTM further suggests that if a rigorous measure of the total pore space is desired, this can only be obtained by determining absolute specific gravity by first reducing the sample to discrete particles, each of which is sufficiently small so that no impermeable pore space can exist within any of the particles. For this purpose, a core specimen obtained from a model concrete slab section (block) made from batch #35 was sliced, using a low-speed saw with special blade, in six thin discs having average diameter of 18.44 mm and thicknesses ranging from approximately 1 mm to 21 mm. Following the procedure stipulated by ASTM, the total pore space in each disc of concrete specimen was estimated to range from about 20%, for the 1 mm slice, to approximately 8%, for the 21 mm disc, giving an average of 11.37% of permeable pore space for the entire core specimen as shown in Table 3.1. This method required three additional days for the preparation of the thin disc-specimens before the 5-day standard procedure stipulated by ASTM C642 was employed. From the above results, it can be concluded that the ASTM C642 method provided a sufficiently good estimate, within about 1%, of the volume of permeable pore space (voids) of the hardened concrete produced by the batches under investigation.

### 3.5.3 Permeability vs. Porosity

From the results obtained from the above experiments, one would expect that the concrete specimen which had the lower percent of void content would logically exhibit a lower water permeability since the total permeable pore space was smaller. These same concrete specimens were previously used in the laboratory permeameter and their corresponding permeabilities were determined to be 9.503E-12 cm/sec and 6.94E-12 cm/sec for batch #33 and #35, respectively. It is interesting to note that although the specimen from batch #35 had approximately 27% more permeable pore

Table 3.1 Estimation of Permeable Pore Space (Effective Porosity) in a Hardened Concrete Specimen

Specimen (DISC) No.	Measured Diameter (mm)	Measured Thickness (mm)	Volume of Solid, $V_s$ (incl. Pore Space) $\times E_4(cc)$	Oven-Dry Weight, $W_0$ (g)	Saturated Surface Dry Weight, $W_{SSD}$ (g)	$W_{SSD} - W_0$ (g)	Volume of Pore Space, $V_p$ $\times E_6(cc)^p$	Permeable Pore Space, (Effective Porosity)
1	18.41	1.06	2.82	0.64	0.67	0.03	55.87	0.198
2	18.45	1.20	3.21	0.70	0.72	0.02	37.24	0.116
3	18.44	2.28	6.09	1.45	1.48	0.03	55.87	0.0917
4	18.44	4.71	12.58	2.96	3.03	0.07	130.35	0.1036
5	18.45	7.72	20.64	4.77	0.67	0.10	186.22	0.0902
6	18.45	21.10	6.35	13.20	13.45	0.25	465.55	0.0826

Room (Air) Temperature = 69°F (20°C)

Water Temperature = 212°F (100°C)

Boiling (Immersion) Time = 30 min.

Density of Concrete Tested = 537 g/cc

Average Effective Porosity = 0.1117 (11.37%)

$$V_p = (W_{SSD} - W_0)/(537 \text{ g/cc})$$

$$\text{Permeable Pore Space (Effective Porosity)} = V_p/V_s$$

space than that of batch #33 it exhibited a 36.93% lower coefficient of permeability. Apparently, the total permeable pore space could not provide a reliable index for the permeability of hardened concrete unless additional parameters which contain more information about the pore structure were available. This clearly indicates that indeed the permeability of concrete is not a simple function of its porosity but depends on the size, distribution, and continuity of the pores - microscopic parameters that are not easy to determine. From the analysis of the limited data available, it appears that no definite correlation between porosity and permeability can be established at this point.

### 3.6 Investigation on the Effective Radius of Flow Region

#### 3.6.1 Concept of Effective Radius of Flow Region

An attempt was made in order to estimate the effective radius (radius of influence) of the flow region encountered in the field permeability test. Although the flow region is difficult to be established, since the boundary conditions are not defined due to the existence of an unsaturated-saturated condition of the moving boundary (flow front), a reasonable estimate of the effective radius could be obtained using the modified Thiem equation used in partially penetrating wells [30]. If it is assumed that the initial radial flow of water into the concrete is similar to that encountered in confined aquifers, then the following equation can be used:

$$Q = 2\pi K L_e (H - h_w) / \ln(r_e/r_w)$$

where  $Q$  = flow from the partially penetrating well

$K$  = hydraulic conductivity (permeability)

$L_e$  = length of the open portion of the well through which flow occurs

$H$  = hydraulic head at a specified distance from center of well  
 $h_w$  = head at the center of well  
 $r_w$  = radius of well  
 $R_e$  = effective radius of the flow system over which the head difference ( $H-h_w$ ) is dissipated

Solving the above equation with respect to  $R_e$ , we get

$$R_e = e^{[2\pi L_e(H-h_w)(K/Q) + \ln(rw)]}$$

It can be recognized that the parameters of this equation are analogous to the ones employed in the FPT; i.e.,  $L_e$  is analogous to the length of test section  $L$  through which flow occurs,  $r_w$  is analogous to the radius of the drilled test hole  $r$ ,  $h_w$  is analogous to the applied constant head (pressure), and  $Q$  is analogous to the volumetric flow of water into the concrete measured during an FPT. By knowing the values of  $K$  and  $Q$ , the effective radius  $R_e$  of the flow region can be estimated. The coefficient of permeability as determined by Darcy's law in the laboratory permeameter is assumed to be the theoretical  $K$  value of the concrete material tested. Then, by using the  $Q$  value obtained from the FPT, and assuming the head  $H$  to be zero,  $R_e$  can be determined using the above equation.

An average value of  $R_e = 1.194$  cm was obtained when  $K$  and  $Q$  values of several batches were used. This indicates that the average depth of penetration of water during a typical FPT run is theoretically around 1 cm into the concrete.

### 3.6.2 Relating Volume of Flow to Volume of Saturated Solid Material

Theoretically, the total volume of water ( $Q$ ) injected into the concrete during an FPT should be equal to the volume of the saturated pore space of the solid material ( $V_e$ ) within the effective flow region, provided that the material is fully saturated. Having estimated the porosity of the concrete material, an equivalent cylindrical volume of saturated solid (not including any void space) can be calculated. The volume of saturated solid  $V_{s.s.}$  (including voids) can be calculated by subtracting the volume occupied by the test hole. Finally, the  $V_e$  can be calculated by multiplying  $V_{s.s.}$  by the porosity.

#### Example: Batch #35

$$\text{Total } Q = 0.359 \text{ cc}$$

$$\text{Porosity} = 12.30\% \text{ (estimated volume of permeable space)}$$

$$\Rightarrow \text{Equiv. Cyl. Vol. of Sat. Solid} = 0.359 \text{ cc} / .1230 = 2.919 \text{ cc}$$

### 3.6.3 Estimation of Permeability Based on Effective Radius of Flow Region

If the effective radius of flow region is properly estimated, then the modified Thiem equation presented above can be solved with respect to  $K$  and used to obtain an estimate of the permeability. However, in order to obtain an accurate and sufficiently precise value of  $R_e$ , a sophisticated finite-element computer model, able to handle unsteady initial flow condition with progressing unsaturated-saturated interface of a moving boundary, is required. Such a computer model is not readily available. An additional limitation is that the porosity of the tested concrete should also be known. This parameter is not easily obtained, and there does not exist any method to determine the porosity of large structural concrete elements such as those tested in the field.

### 3.7 Test Procedure

Using the newly developed prototype FPT instrument, it is now possible to test structural concrete at the site and under actual field conditions rather than coring a sample from a structure and bringing it to the lab for analysis.

The finalized FPT apparatus consists of two main units, namely, the FPT probe which is the actual device that is inserted into the test hole and which injects pressurized water into the concrete mass, and the FPT instrumentation unit which provides the central control and the monitoring during a field permeability test run.

In situ permeability tests can be run at different locations on the structure. Structural elements such as pile columns, piers, and pier/pile caps of bridge substructures can be selected for testing based on needs, available data, field inspection and evaluation of the condition of the site concrete, and accessibility of test location. The concrete to be tested should be sound and without any signs of deterioration (scaling, cracking, spalling, corrosion, etc.), and the concrete surface should be cleaned from any marine organisms if the selected test location is within the tidal or splash zones. The field permeability test is performed by inserting the FPT probe in a 7/8-inch diameter, 8-inch deep hole drilled perpendicular to the concrete surface (the relative location of the reinforcing steel and the clear concrete cover should be determined before any drilling is performed by using a portable R-Meter to avoid altering the structural integrity of the concrete element tested), sealing off a section of the hole with the double-packer mechanism of the probe, and applying high pressure to force the water to permeate radially into the concrete mass. The rate of flow of water into the test section, i.e., the

injection rate, is constantly monitored by means of the manometer set-up mounted on the upper shell of the FPT instrumentation unit. Measurements are taken at regular time intervals and as long as it takes to obtain uniform readings within acceptable limits. By determining the average volumetric flow (cc/sec) of water into the concrete a permeability value can be calculated using the Packer (Lugeon) equations. The moisture content of the concrete at the test location is measured before, during, and after testing using a nondestructive portable moisture meter (M-49 H<sub>2</sub>O Meter) in order to determine the initial condition of the tested section as well as to determine whether the FPT probe is properly injecting water into the surrounding concrete mass.

Usually, a higher rate of flow into the concrete mass is obtained when the concrete is dry, as compared to the ones obtained when the concrete is partially or fully saturated. In such a case, a high initial drop of the water level in the manometer tube is observed. However, the flow should resume normal rates after the initial drop is accounted for. In order to eliminate any test discrepancies due to the above, as well as to offset any possible effects due to conditions such as capillarity and absorption, the test procedure which is followed is to allow the water to flow into the concrete for approximately 30 minutes and then to begin regular flow measurements. The step-by-step FPT operating and testing procedure employed in this study is presented in detail in Appendix A.

### 3.8 Method of Analysis of Data

The developed method of analysis is short and simple, and does not require any complicated calculations or the use of any sophisticated statistical approach. The simplification of the analytical equations along

with the proper reduction of empirical data can produce the desirable results rapidly and easily. The use of computer is not required but is recommended only in the case that an optional graphical representation of the obtained test results is desired. Otherwise, a hand-held calculator is sufficient for the required calculations since all the constants and conversion factors are provided.

The developed procedure consists of three stages, namely, data collection, data reduction and analysis, and determination of the permeability index. These are presented in the following sections.

### 3.8.1 Data Collection

Field permeability test data performed on in-service concrete structures should be recorded in a standard data sheet as shown in Figure 3.8. The geographical location or orientation of the structure to be tested with respect to other highway facilities or routes is a useful information that could be recorded for possible future reference. Reference coding or numbering of the structural element tested should be utilized. Although any arbitrary coding system could be used, it is recommended that a conventional system which is either previously used by the testing agency or one that corresponds to the design of the structure would offer a more convenient reference. Exact recording of the test location is very important. A visual documentation such as a photograph or a schematic diagram is the best record. This should clearly indicate whether the test section is within or above the splash zone in case, for example, the structural element is a submerged pile. If this is not possible, a reference to the distance of the test hole from the high-tide level is an alternative sufficient information.

**FIELD PERMEABILITY TEST (FPT)  
DATA SHEET**

Figure 3.8 Standard FPT Data Sheet

The percent relative moisture of the in situ concrete should be recorded before and after any test is performed. Readings at the four diametrical points around the test hole should be taken, and recorded along with the average value. Finally, the applied test pressure and the starting time of test measurements should be recorded before an actual FPT is performed according to the test procedure described in section 3.7. Any problems, anomalies, discontinuities, or disruptions that may occur during a test run should be recorded under "Remarks" on the FPT Data Sheet.

Measurements can be taken at any selected convenient regular time interval between 5 to 15 minutes and as long as it takes to obtain uniform readings within acceptable limits. For each time interval, the change of the water level in the manometer ( $\Delta H$ ) is measured and recorded in the appropriate column on the data sheet. If for a fixed time interval, a measurement of  $\Delta H$  which is within the precision of the measuring device is repeatedly recorded for at least a total of 30 minutes, then this would indicate that a relatively constant injection rate is achieved. For all practical purposes, this would also indicate that a steady-state flow condition is reached, and the test run is thus completed.

In addition to the data recorded on the FPT Data Sheet, for each concrete structure tested the following information should be obtained, if possible:

- a) The design service life of the structure.
- b) The age of the structure.
- c) The distance from the coast.
- d) The concrete type used and any available mix design parameters.
- e) The thickness of concrete cover over the reinforcing steel.

- f) Other protection for the reinforcing steel bars such as epoxy coating or cathodic protection systems.

### 3.8.2 Data Reduction and Analysis

The data reduction process involves the conversion of the obtained raw measurements of the drop of the water level ( $\Delta H$ ) in the manometer to a volumetric flow in cubic centimeters (cc) and then to an average rate of water inflow (injection rate) in cc/sec.

This is demonstrated in the following simple example:

Applied test pressure,  $P = 200$  psi

FPT measurement time interval = 10 minutes

Constant drop of water level in the manometer,  $\Delta H = 0.5$  inches

The inside diameter of the manometer tubing is known and assumed to have a constant value of  $d = 0.078$  inches. By simple geometry, a cylindrical volume is obtained by multiplying by  $(\pi \times d^2/4)$ . Since the measurements are more conveniently taken in inches, the constant factor  $C_c = 0.07830333$  is used to directly convert cubic inches to cubic centimeters (cc). Therefore, for this example, the total volume of water injected into the concrete per 10-minute interval is simply  $V_q = C_c \times 0.5 = 0.03915$  cc, which is, in turn, converted into a constant rate of flow,  $Q = 6.525E-5$  cc/sec by dividing  $V_q$  by the time interval. Although cubic inches per seconds could also be used to express the value of the rate of flow, it is more customary to report this parameter in the literature using the SI-units of cubic centimeter per seconds (cc/sec).

There are two basic approaches for analyzing the reduced FPT data. In the case where a steady-state flow condition has clearly been established during an FPT run (i.e., a constant value of  $\Delta H$  repeatedly recorded for at least 30 minutes), then the measured injection rate automatically

defines the constant rate of flow of water into the concrete (cc/sec). In the event where the obtained measurements do not clearly indicate a steady-state, then the cumulative volume of water (cc) injected into the concrete is graphically plotted versus the total test time elapsed. The slope of the produced curve at any point indicates the rate of flow (volume per unit of time) of water into the concrete at the corresponding test time. For each FPT data set plotted, an average rate of inflow can be determined where the produced curve is approximately linear (i.e., the slope of the curve is approximately constant). Five to seven data points of the linear portion of the obtained plot, usually corresponding to the final 15 to 30 minutes of testing, should be considered in determining the reported average inflow. Figure 3.9 is a typical plot of actual FPT data analyzed in such a manner.

### 3.8.3 Determination of Apparent Permeability Coefficient

Once a rate of flow of water injected into the concrete tested is established, a permeability coefficient can be determined by using the Packer/Lugeon equations presented in Section 3.4. Since the length of the test section,  $L_0$ , is fixed and constant for every test, and its value always lies between  $r$  and  $10r$ , Equation 3.10A is, therefore, applicable for the FPT set-up employed in this study. A close study of this equation reveals that the only variable in this case is the rate of flow,  $Q$ , which is the measurable parameter determined from the FPT data. Since the pressure is set to a constant level during each test, the equation can be further simplified by incorporating every term into a constant factor " $C_k$ " which has a value of  $63.134E-5$ . The permeability index is thus determined by simply dividing the measured rate of flow (cc/sec) by the pressure

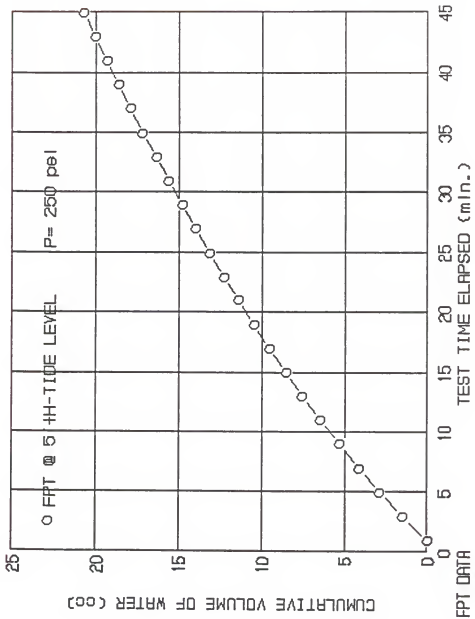


Figure 3.9 FPT Measurements from B. B. McCormick Bridge, Jacksonville

value expressed in units of "psi" and then multiply the output by the constant  $C_k$  to directly obtain the permeability index in units of cm/sec. For the particular example presented in the above section, the permeability index is determined as follows:

$$K = (Q/P) \times C_k = (6.525E-5/200) \times 63.134E-5 = 2.06 \times 10^{-10} \text{ cm/sec}$$

Therefore, the apparent permeability coefficient for the concrete tested is thus determined to be equal to  $2.06E-10$  cm/sec. By simply dividing this value by a factor of 2.54 cm/in, the result may optionally be obtained in units of in/sec. Since this permeability value is without any possible adjustment or correction, it is referred to as the "apparent" permeability coefficient ( $K$ ).

CHAPTER 4  
EVALUATION OF THE DEVELOPED FPT APPARATUS AND METHOD

4.1 Laboratory Experimentation

**4.1.1 Evaluation of the Sealing Mechanism of the FPT Probe**

An evaluation of the developed FPT device was performed in order to assure that the new design of the sealing mechanism could operate properly. The new probe was assembled inside a 1-inch-thick-walled aluminum pipe and repeatedly subjected to externally applied pressures as high as 1,400 psi. The probe was then used in a number of laboratory trials performed on concrete specimens at various pressure levels and different test orientations (vertical, horizontal and inclined at various angles). The FPT probe performed satisfactorily, and no leakage or any other problems were encountered during this experimentation.

**4.1.2 Evaluation of the FPT Instrumentation Unit**

The FPT instrumentation unit was extensively tested, and the pressure regulator and test gauge were properly calibrated. All the parts and connections of the unit were high-pressure-tested for safety, and the operation of the individual components was thoroughly checked. The completed instrumentation unit was repeatedly used in a number of laboratory tests, and demonstrated satisfactory performance with no problems encountered in any of the tests. The developed instrumentation unit enabled an efficient operation of the FPT apparatus by simplifying the test set-up and dismantling of the apparatus and, thus, drastically reducing the time required for performing the FPTs.

#### 4.1.3 Performance of the FPT Apparatus Under Long-Term Testing

An evaluation of the performance characteristics of the FPT apparatus under long-term laboratory testing was performed. The FPT apparatus was subjected to more than 1,500 hours of continuous operation under an externally applied pressure of 500 psi in the laboratory. Extensive monitoring was carried out, and no leakage, disruption, or any other anomalies were observed at any stage of the operation. Based on the above evaluation it was concluded that the sealing mechanism of the device works satisfactorily for even prolonged periods of operation and that the developed FPT apparatus can also be effectively used as a long-term testing device in the laboratory.

#### 4.1.4 Effect of Test Orientation

The effect of test orientation on the obtained FPT measurements was also investigated. FPTs were performed on concrete slab sections (blocks) in vertical, horizontal and inverted positions. Figure 4.1 is a typical plot of cumulative flow versus test time elapsed obtained during this experimentation. The slope at every point on the curve corresponds to the rate of flow of water (cc/min.) into the concrete. The last four points of the linear portion of each curve, corresponding to the last six minutes of each test run, were considered to determine the average flow for each boundary condition. The average flows obtained from FPTs performed at these orientations on eight concrete test blocks are tabulated in Table 4.1. As can be seen from the slopes of each curve in Figure 4.1 and the values in Table 4.1, the test flows obtained from each boundary condition corresponded closely to each other. This indicates that test orientation does not appear to have a significant effect on test results, and gravitational effects on the measured flow rates due to orientation, if any, appear to be negligible.

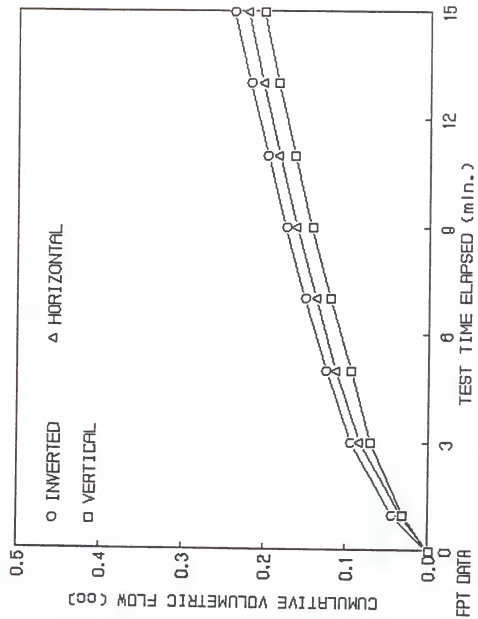


Figure 4.1 Typical Flows Obtained from FPTs Performed at Different Test Orientations

Table 4.1 Effect of Test Orientation on Flow Rate in the FPT

TEST ORIENTATION	A V E R A G E   V O L U M E T R I C					F L O W (cc/min.)		
	B33/SP2*	B44/SP2	B45/SP2	B47/SP2	B48/SP1	B94/SP2	B48/SP1	B97/SP1
INVERTED	0.039	0.014	0.009	0.036	0.016	0.0028	0.0063	0.028
HORIZONTAL	0.037	0.012	0.009	0.036	0.015	0.0026	0.0067	0.027
VERTICAL	0.035	0.012	0.007	0.036	0.017	0.0028	0.0067	0.028

Key: \* B/SP = Indicates Concrete Batch and Specimen Numbers

#### 4.1.5 Effect of Using a Partially Filled Test Section

Another set of laboratory experiments was carried out in order to determine if a partially filled test section at the initial stage of a test would have any effect on the measured flow rates. For this purpose the FPT probe was assembled in a cylindrical transparent acrylic tube which allowed continuous observation of the sealed test section in any orientation. A syringe with hypodermic needle was then used to introduce water into the sealed test section of the tube. The 2-inch test section was divided into 6 levels which were marked on the acrylic tube. The volumetric quantity of water required to fill the test section to each prescribed level was measured several times and the average was recorded as shown in Table 4.2. The FPT probe was then assembled in a drilled hole in concrete blocks. For each test run, the test section was filled up with the predetermined volumetric quantity of water required for each level. Regular FPTs were then performed, and the initial head drop of the water level in the manometer tube was measured and recorded as shown in Table 4.3. When the test section was completely filled with water, the water meniscus in the manometer tube maintained its original position and no drop of water level was registered at the initial application of pressure, since water is incompressible. In cases where the test section was not completely filled with water, the initial drop of water level in the manometer tube corresponded closely to the quantity of water required to be added to that level in order to completely fill the test section as a comparison of the volumetric values in Tables 4.2 and 4.3 indicates. It was concluded that, since the FPT set-up was a closed-system and no leakage occurred during a test, the initial drop of water level was a clear indication that the test section was not completely filled with water at

Table 4.2 Volumetric Quantity of Water Required to Fill the Test Section

PORTION OF TEST SECTION FILLED	MEASURED VOLUME OF WATER (cc)
6/6	13.2
5/6	10.9
4/6	8.8
3/6	6.5
2/6	4.3
1/6	2.3

Table 4.3 Volume of Water Corresponding to Initial Head Drop in Manometer

BATCH/SPECIMEN No.	PREDETERMINED LEVEL OF TEST SECTION FILLED	INITIAL HEAD DROP IN THE MANOMETER (in.)	CORRESPONDING VOLUME OF WATER (cc)
B100/SP3	5/6	NOT REGISTERED	N/R
	5/6	31.25	2.447
	4/6	63.25	4.953
	4/6	86.75	9.200
	2/6	117.5	9.200
	1/6	145.0	11.353
B29/SP2	6/6	0.25	0.019
	5/6	25.625	2.007
	3/6	76.50	5.99
B29/SP3	6/6	N/R	N/R
	4/6	45.25	3.543
	2/6	99.75	7.811
	1/6	135.25	10.591

Table 4.3--continued.

BATCH/SPECIMEN No.	PREDETERMINED LEVEL OF TEST SECTION FILLED	INITIAL HEAD DROP IN THE MANOMETER (in.)	CORRESPONDING VOLUME OF WATER (cc)
B31/SP1	6/6	N/R	N/R
	5/6	29.50	2.310
	4/6	61.75	4.855
	3/6	89.75	7.028
B35/SP1	6/6	N/R	N/R
	5/6	26.75	2.036
B36/SP1	6/6	N/R	N/R
	5/6	33.00	2.584
B44/SP2	4/6	57.75	4.522
	3/6	82.25	6.441
B42/SP2	6/6	0.5	0.0098
	5/6	28.5	2.231
	4/6	89.75	4.522
B44/SP1	6/6	N/R	N/R
	5/6	26.00	2.036
	3/6	57.75	4.248
B44/SP2	6/6	N/R	N/R
	3/6	87.75	6.871
B47/SP1	6/6	0.125	0.0098
	1/6	142.08	11.125
B48/SP1	6/6	N/R	N/R
	5/6	33.875	2.653
	4/6	56.25	4.405

the beginning of a test. However, it was observed that after the first few minutes (1-3 min.) of testing and the initial head drop in the manometer was accounted for, the flow of water injected into the concrete resumed regular rates. Therefore, in case that the application of a vacuum happens to be ineffective, a recommended practice is to allow the water to initially fill any empty portion of the sealed test section, and then to begin the flow measurements after a regular flow is achieved. Based on the above experimental data, it can be concluded that a partially filled test section at the initial stage of the test should not have any effect on the obtained final flow rates.

#### 4.1.6 Effect of Initial Condition of Concrete

Three different initial conditions of the test sections were employed in this study: (I) Dry, (II) Partially Saturated, and (III) Saturated. Since the flow characteristics of oven-dried and air-dried test specimens produced similar results, the air-drying method was adopted in this study to simplify and accelerate the test procedure. To obtain condition (I), the concrete slab was left to dry in the permeability laboratory for at least one week, and prior to testing, the test section was dried with a hand held hair dryer. Condition (II) was achieved by filling the test section with water for 24 hours prior to testing. Condition (III) was obtained when the test section had already been subjected to an FPT within the last 24 hours. A total of eight concrete test blocks were used for this experimentation.

Generally, a higher flow rate into the concrete mass was obtained when condition (I) was used, as compared to (II) and (III). This is shown in Figure 4.2. The interesting result from these tests was that comparative flow rates (i.e., relatively constant sloped curves) were obtained if the test section was either pre-saturated (condition II), or pre-tested

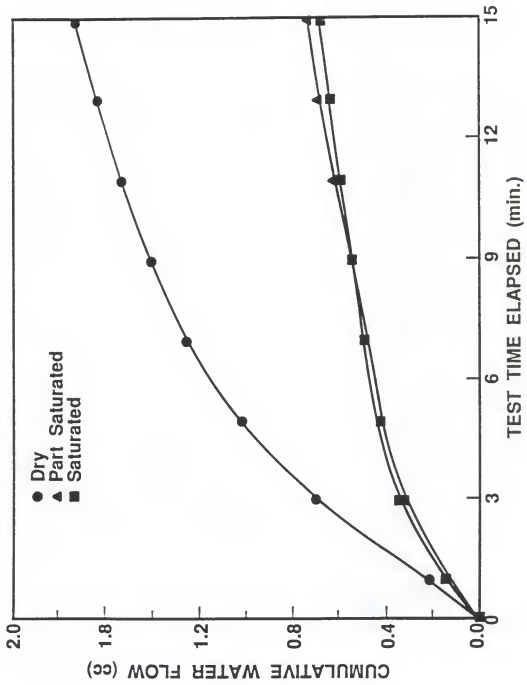


Figure 4.2 Typical FPT Flows Indicating the Effect of Initial Condition of Concrete

(condition III) using the device as shown in Figure 4.2. The test measurements obtained from these experiments are summarized in Table 4.4. The average flows were computed in the same manner as previously described in section 4.1.4. Comparison of test measurements obtained from conditions (I) and (III) showed a high variation ranging from about 63% to 203% while the variation between conditions (II) and (III) ranged between 0% to about 58%. This indicates that the initial condition of concrete has a significant effect on the FPT measurements. Therefore, a vacuum preconditioning and subsequent pre-saturation of the test section prior to testing is recommended in case the concrete to be tested is relatively dry.

#### 4.1.7 Effect of Applied Test Pressure

According to Darcy's law, the flow of water through a porous medium is directly proportional to the applied pressure head when all other parameters remain constant. This is also reflected in the Packer/Lugeon equations (Eq. 3.10A and 3.10B) used in the developed FPT method. In order to verify that the experimental results obtained using the FPT method reflect this theoretical relationship the effect of the applied test pressure on these results was investigated.

A series of FPTs were performed over several days on a randomly selected concrete test block which was previously saturated in a water container for a total duration of 11.5 months in the laboratory. This test block was casted on 4/5/88 from concrete batch #32 prepared in the main laboratory testing program. The mean 28-day compressive and splitting tensile strengths were determined to be 7,058 psi and 601 psi, respectively, for this particular concrete mix [31]. Repetitive FPTs were performed at various levels of applied test pressure, starting at 100 psi and progressing to higher levels in increments of 50 psi until the

Table 4.4 Effect of Initial Condition of Concrete on Flow Rate in the FPT

INITIAL CONDITION OF CONCRETE	A V E R A G E			V O L U M E T R I C			F L O W (cc/min.)		
	B30/SP1	B32/SP3	B37/SP2	B38/SP1	B39/SP2	B40/SP3	B41/SP1	B43/SP1	
DRY	0.0333	0.0225	0.0057	0.0857	0.0363	0.1623	0.0298	0.0245	
PART. SATURATED	0.0175	0.0085	0.0057	0.0592	0.0270	0.1077	0.0160	0.0167	
SATURATED	0.0110	0.0078	0.0057	0.0442	0.0205	0.0857	0.0110	0.0150	

Key: B/SP = Indicates Concrete Batch and Specimen Numbers.

concrete block was fractured. All the other test parameters were kept constant. FPTs were performed on the concrete specimen while submerged in water for safety reasons and in order to readily detect any leakage. The coefficient of permeability was determined at each test pressure level using Equation 3.10A. The obtained experimental values are summarized in Table 4.5.

As it is indicated in Table 4.5, the concrete test block failed (fractured) at an applied test pressure of 900 psi, which was 49.75% higher than the 28-day mean splitting tensile strength, and which corresponded to 12.75% of the 28-day mean compressive strength of the particular concrete mix used in this experimentation. The mean coefficient of permeability, as determined by the FPT method at the range of applied test pressure between 100 psi to 700 psi, was 9.898E-12 cm/sec, with a sample standard deviation of 0.85982E-12cm/sec and a coefficient of variation (C.V.) of 8.687%. This value was about 11.7% higher than the mean coefficient of permeability of 8.86E-12 cm/sec determined from cylindrical specimens of the same concrete batch tested in the laboratory permeameter [31]. A large increase in flow measurements was observed at test pressures between 750 psi to 850 psi which produced a mean coefficient of permeability of 35.653E-12 cm/sec, which was about 260% higher than the mean permeability as determined from FPTs performed within the 100 psi to 700 psi pressure range. Figure 4.3 is a graphical representation of the test results obtained from this experimentation.

As can be seen from the experimental values presented in Table 4.5 and Figure 4.3, relatively consistent permeability results were obtained using the FPT apparatus on concrete which was previously saturated for a prolonged period of time and which was tested at applied pressures as high

Table 4.5 Coefficient of Permeability Determined at Different Applied Test Pressure

APPLIED TEST PRESSURE (psi)	COEFFICIENT OF PERMEABILITY (x E-12 cm/sec)
150	7.65
150	10.79
200	9.95
250	9.87
300	10.65
350	9.67
150	9.28
450	10.79
500	9.95
550	9.16
600 *(TENSILE)	10.65
500	10.05
700	10.84
750	22.91
800	35.14
850	48.91
900 (FAILURE)	-----

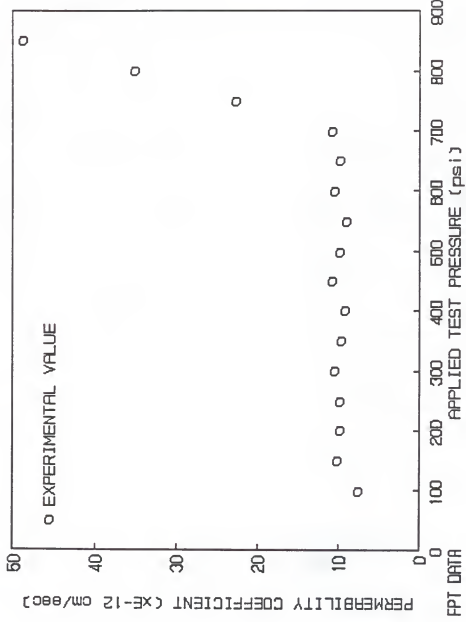


Figure 4.3 Plot of Coefficient of Permeability Determined by FPTs Performed at Different Applied Test Pressure

as 10% of its 28-day mean compressive strength. Therefore, it can be concluded that the applied test pressure should not have any significant effect on the produced FPT results provided that the concrete tested is sound and no leakage occurs during the test. However, since at this point only limited data have been obtained, it is recommended that test pressures be kept to a minimum level adequate to produce a measurable flow during an FPT run in order to avoid the risk of causing any internal cracking to the concrete tested.

#### 4.1.8 Flow Characteristics of FPT Under Long-Term Testing

Test data had previously indicated that, if the test concrete is close to a saturated condition, the coefficient of permeability as determined by the FPT method would correspond closely to that obtained with the laboratory permeameter [31]. Since the controlling test variable to achieve a saturated condition is time, the flow characteristics of the FPT under long-term testing were examined.

An initially oven-dried concrete test block made from batch #36 was immersed in a water bath for 21 days prior to testing and subsequently subjected to an FPT. The coefficient of permeability was determined from the FPT measurements at different time intervals during the continuous testing and plotted versus the elapsed test time as shown in Figure 4.4. As expected, the measured coefficient of permeability was observed to change with time until a fully saturated, steady-state flow condition was reached. In other laboratory experimentations using the FPT, a steady-state flow condition was usually reached within approximately 2 hours from the commencement of an FPT when concrete test blocks which were previously saturated in water for a year were used. For the particular concrete specimen tested in this case, it took approximately 11 days to reach a steady-state flow at an applied pressure of 300 psi. The test run was

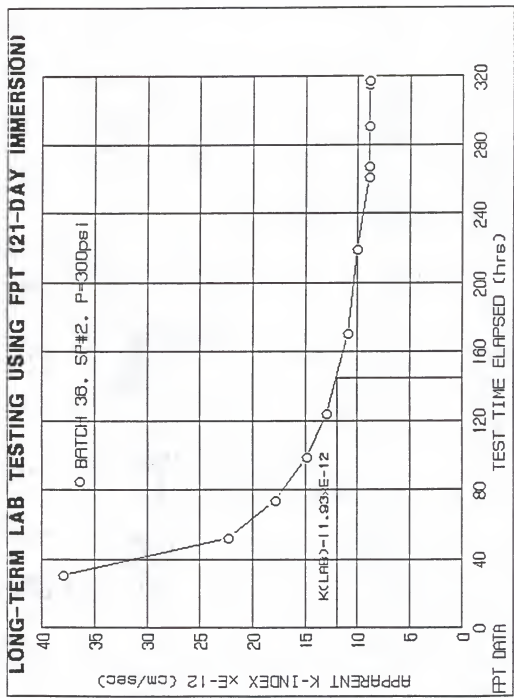


Figure 4.4 Plot of FPT Results Obtained from Long-term Laboratory Testing

continued for an additional 48 hours after the steady-state condition to a total of 13 days in order to assure that a steady-state flow region was established in the plot of permeability versus time. The coefficient of permeability finally obtained in this manner was approximately 34% lower than the mean coefficient of permeability determined by testing cylindrical specimens obtained from the same concrete batch in the laboratory permeameter [31], as indicated in Figure 4.4.

#### 4.1.9 Evaluation of Repeatability of the FPT

The FPT method has been evaluated for its repeatability as well as its reproducibility in a previous research study [23,31]. From the obtained results, which had a coefficient of variation (C.V.) ranging from approximately 2 to 8 percent, it was concluded that the developed FPT method produced results with acceptable uniformity and demonstrated adequate repeatability for the purpose of the study. Repeatability refers to acceptable uniformity of test results obtained on the same sample by the same tester (experimenter) and with the same equipment. Since most of the variance was attributed to differences in moisture content, it was decided to perform an evaluation in order to determine if a "within-test" variation would have any significant effect on the repeatability of the FPT. This was determined as follows:

Repetitive tests on concrete blocks, having different initial condition of the concrete material (i.e., dry, partially saturated, and saturated), were performed using the FPT method. A total of three 15-minute sequential tests were performed for each condition. After the first set of measurements was completed, the test run was interrupted by closing the test pressure valve, removing, refilling and connecting the test tubing back to the FPT probe, then resetting and subsequently resuming regular

measurements for a second test run while the test device (FPT probe) was still assembled in the test section of the concrete specimen. The same sequence of steps was followed with the important difference that this time, at the end of the second test run, the device was dismantled and removed from the concrete specimen; the test section was flushed clean and refilled, and then the FPT probe was assembled back into the test section prior to the resumption of the third sequence of test measurements. The purpose of this testing procedure was to determine whether a simulated "within-test" variation, such as the interruption of testing and the removal of the device from the test section between sequential test runs, had an effect on the repeatability of the FPT. The cumulative volume of water injected into the concrete material versus the test time elapsed was plotted for each test as shown in Figures 4.5 and 4.6. As it can be seen from these figures, comparative flow responses i.e., curves of relatively constant slopes, were obtained whether or not the device was removed from the test section between sequential test runs (see Test #2 and Test #3 curves). Therefore, it was concluded that, for the purpose of this study, any "within-test" variation had no significant effect on the repeatability of the FPT. It is noticeable that for the same test time elapsed, a larger cumulative volume of water was injected into the test section if the concrete material was initially dry as opposed to partially saturated, as it was previously explained in Section 4.1.6. However, a closer examination of Figures 4.5 and 4.6 reveals that the respective slopes of the curves for Test #2 and Test #3 in each figure correspond closely to each other. This was a typical response obtained in all the tests performed during this evaluation. Therefore, it can be inferred that a "within-test" variation of this nature should not have a significant effect on the

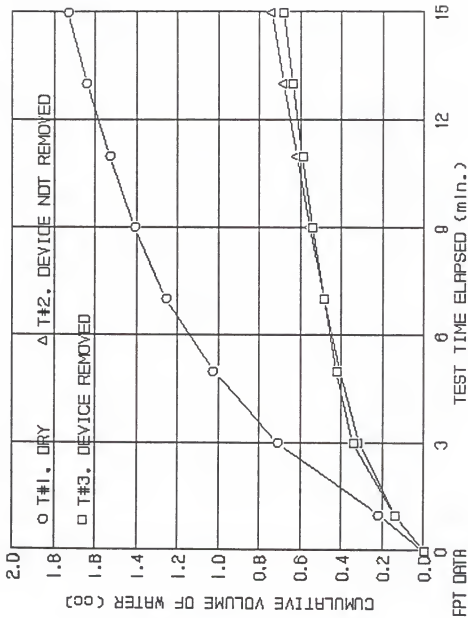


Figure 4.5 Typical Plot Indicating the Repeatability of the FPT Method When the Concrete is Dry

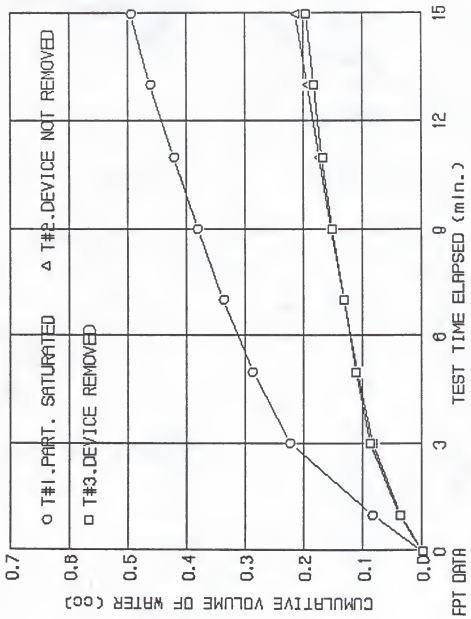


Figure 4.6 Typical Plot Indicating the Repeatability of the FPT Method When the Concrete is Partially Saturated

repeatability of the results produced by the FPT method provided that all the other parameters remain constant.

#### 4.1.10 Correlation Between FPT and Lab Permeability Test Results

The coefficients of permeability as determined by the FPTs on concrete test blocks were compared with those obtained by an existing laboratory permeability test method, which was developed by Soongswang et al. and had been shown to produce reliable results [32]. In this laboratory test method, the rate of flow of water through a cylindrical concrete specimen 4 inches in diameter and 2 inches in height under a pressure of 100 psi is used to determine the coefficient of permeability by a direct application of Darcy's law. The laboratory permeability tests were run on concrete specimens made from the same batches of concrete for the concrete blocks, and moist-cured for 28 days. Figure 4.7 shows the plot of the average coefficient of permeability as determined by the FPTs,  $K_{FPT}$ , against the average permeability coefficients as determined by the laboratory method,  $K_{LAB}$ , for the same batches of concrete. Analysis of test results indicated that the values of the coefficients as determined by the FPT method were 70% higher than the values obtained by the laboratory method ( $K_{FPT}/K_{LAB}=1.70$ ) for the respective concrete mixtures tested [23,31]. A correlation analysis between the results of the FPT and laboratory test was performed using linear regression. The results of the regression analysis were as follows:

$$K_{FPT} = 1.719 K_{LAB} - 0.2106 \quad (4.1)$$

Number of Observations = 7

Standard Error of the Slope = 0.155793

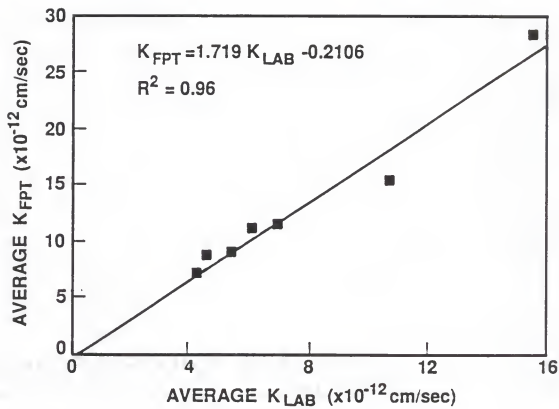


Figure 4.7 Correlation Between the Results of the FPT and the Laboratory Permeability Test

A coefficient of determination ( $R^2$ ) of 0.96 was obtained, indicating that the relation between the two methods is highly significant. The regression equation has a slope of 1.719, as shown in Figure 4.7. The relatively high percent difference in the results obtained by the two methods might be due to the fact that the concrete blocks tested by the FPT method were partially dry while the cylindrical specimens tested in the laboratory permeameter were fully saturated prior to testing. As presented earlier in Section 4.1.6, the initial condition of concrete prior to testing has a significant effect on the FPT results. In addition, the specimen-to-specimen differences such as shape and size might have had an effect on the test results.

The empirical correlation between the experimental values obtained by these two test methods was further examined by performing FPTs on 10 additional concrete blocks which were randomly selected from the same laboratory produced concrete batches. However, the difference in this series was that the concrete blocks tested were previously saturated by immersion in water for a total duration of one year, and subsequently tested using the FPT while submerged in the water. The results from these FPTs are presented in Table 4.6 along with the permeability values as determined by the laboratory test method for the respective concrete batches and specimens. In this series of tests, the values of the coefficients as determined by the FPT method were, on the average, 28.7% higher than the values obtained by the laboratory method (average  $K_{FPT}/K_{LAB}$  ratio = 1.2867). Figure 4.8 shows the plot of the coefficients of permeability as determined by the FPTs,  $K_{FPT}$ , against the permeability coefficients as determined by the laboratory method,  $K_{LAB}$ , for the same batches of concrete. A correlation analysis of the results presented in Table 4.6 was performed

Table 4.6 Permeability of Concrete Specimens as Determined by the FPT and Lab Methods

BATCH/SPECIMEN No.	COEFFICIENT OF PERMEABILITY ( $\times 10^{-12}$ cm/sec)		K(FPT)/K(LAB) RATIO
	FPT METHOD	LAB METHOD	
B33/SP1	12.185	8.966	1.359
B33/SP2	11.979	10.109	1.185
B36/SP1	13.410	10.947	1.225
B36/SP2	15.909	12.903	1.233
B39/SP2	24.497	10.947	1.359
B40/SP1	10.020	7.798	1.285
B40/SP2	9.102	7.442	1.223
B48/SP2	17.247	11.506	1.499
B98/SP2	4.523	3.785	1.195
B100/SP1	5.986	4.623	1.295

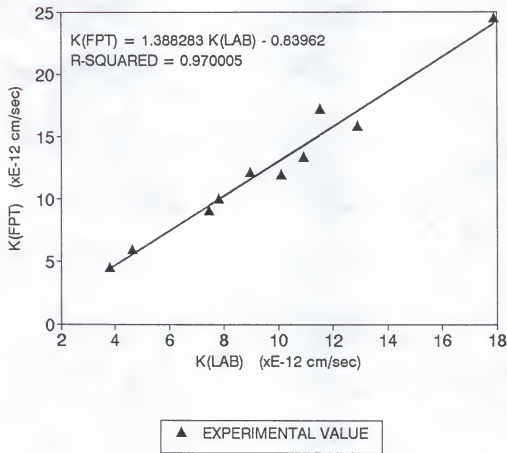


Figure 4.8 Correlation Between the Results of the FPT and Laboratory Permeability Test When Concrete is Saturated

using linear regression. The results of the regression analysis were as follows:

$$K_{FPT} = 1.388283 K_{LAB} - 0.83962 \quad (4.2)$$

$$R^2 = 0.970005$$

$$\text{Number of Observations} = 10$$

$$\text{Standard Error of the Slope} = 0.086311$$

The coefficient of determination ( $R^2$ ) was improved to 0.97 as compared to 0.96 obtained in the testing of the partially dry concrete blocks, indicating that a strong positive relation exists between the two methods. The regression equation has a slope of 1.388, as shown in Figure 4.8. The discrepancies in the results obtained by the two methods might be partially due to the fact that the concrete blocks tested are limited in size, while the analytical equation (Eq. 3.10A) used in the FPT method assumes that the concrete is infinite in dimension. The smaller concrete size might produce a higher flow, and thus a higher computed permeability coefficient. In consideration of the high variability of most permeability test results, discrepancies of such magnitude in permeability coefficient could be regarded as minimal. The closeness of the FPT results to the laboratory permeability test results indicated that the FPT method could produce fairly consistent and reliable test results.

#### 4.2 Field Experimentation

The performance and reliability of the developed FPT apparatus and method were evaluated in numerous field testing operations carried out on in-service concrete structures throughout Florida. A total of thirteen

concrete bridge structures have been tested using the developed FPT apparatus. The major objectives of this field experimentation were (1) to evaluate the performance of the FPT apparatus under actual field conditions as a module of a portable field test unit for the determination of in situ permeability of concrete, and (2) to interpret the test results obtained with the FPT method in order to gain important information on the durability of the concrete structures under investigation. Only the first objective is discussed here. The second objective is covered in Chapters 5 and 6.

FPTs were performed on structural elements of bridge substructures at various locations, elevations, and orientations based on needs and accessibility of test locations. Figure 4.9 shows the FPT probe installed on a partially submerged pile column of an in-service concrete bridge during actual field testing. Flow measurements were remotely taken by means of the FPT instrumentation unit which was carried on and operated from a boat as shown in Figure 4.10. The FPTs were conducted by one person plus an assistant, and test measurements were completed usually within two hours from the commencement of the actual test run. The entire FPT operation including coring, pre-conditioning, testing, and patching of concrete was completed within approximately two to three hours.

The FPT apparatus demonstrated satisfactory performance, and no major problems were encountered during the setting, operation, or dismantling of the FPT apparatus in any of the field installations. The portable FPT unit proved to be a simple and efficient measuring system which could be used for a convenient and rapid determination of the in situ water permeability of structural concrete. The visual and structural damage caused to the concrete was minimal, and repeated tests could be



Figure 4.9 Picture Showing the FPT Probe Installed on a Pile Column of a Concrete Bridge



Figure 4.10 Picture Showing the Use of the FPT Instrumentation Unit in an On-Going Test

performed in the same section. Thus the obtained results can be readily verified at the test site. The pre-conditioning and pre-saturation technique employed in the testing procedure proved to be effective in offsetting any possible effects on the test measurements due to moisture, absorption, or capillary action. Thus, more consistent results were obtained. These results were further used to evaluate the durability of the structural concrete under investigation. The test results from the above field operations as well as the durability evaluation of the tested concretes are presented in Chapter 5.

#### 4.3 Conclusions on the Development of the FPT

##### 4.3.1 General

In the development of a portable, quasi nondestructive device to measure the in situ permeability of in-service concrete, several different designs were attempted, and a number of devices were constructed and evaluated until the current prototype was finally adopted. After months of experimentation, an effective design was achieved, and a suitable FPT apparatus, which satisfies all the design requirements set forth in this study, was fabricated. The developed FPT apparatus relies on the accelerated radial flow of water into the concrete under an externally applied high pressure.

The further refinement and modification to the original FPT probe provided a more simplified set-up and dismantling of the apparatus and, thus, an improved overall design of the device was achieved. The finalized FPT apparatus consists of two main units namely, the FPT probe which is the actual device inserted into the test hole and which injects pressurized water into the concrete mass, and the FPT instrumentation unit

which provides the central control and the monitoring during a field permeability test run. The FPT apparatus is simple and easy to use, and is accompanied by an illustrated user's manual which includes operating instructions and a step-by-step testing procedure.

The developed FPT apparatus was evaluated both in the laboratory as well as in the field under actual in situ conditions and demonstrated satisfactory performance characteristics. It can be concluded that the FPT apparatus and method can provide an effective measuring system for the determination of in situ permeability of structural concrete. Since the double-packer configuration of the sealing mechanism of the FPT probe operates satisfactorily for even prolonged periods of operation, the FPT apparatus can also be effectively used as a long-term testing device of structural concrete in the laboratory.

#### 4.3.2 FPT Method

The developed FPT method is efficient and simple, and does not require any complicated calculations or the use of any sophisticated statistical approach. Once the rate of flow of water injected into the concrete tested is established, a coefficient of permeability can easily be determined by using the Packer/Lugeon equations. The given equations were further simplified by incorporating the terms into a constant factor which is used to directly obtain the coefficient in standard units. This simplification along with the proper reduction of test data can produce the desirable results rapidly. The FPT method produces results with acceptable uniformity and adequate repeatability for the purpose of this study. The use of computer is not required with the FPT but is recommended only in case that an optional graphical representation of the obtained test results is desired. All the constants and conversion factors are provided

for a rapid determination of the in situ permeability of structural concrete.

#### 4.3.3 Analytical Solution

In order to verify the validity of the Packer/Lugeon equations used in the FPT method an analytical solution to the flow phenomenon encountered in the FPT was obtained. The flow problem was examined from the macroscopic point of view and was based on the continuum approach in which no attention is paid to the pores or pore structure of the concrete. The three-dimensional, spherical flow model employed in this study provided the proper analytical solution which constituted the mathematical derivation of the Packer/Lugeon equations thus verifying the validity of the FPT method.

#### 4.3.4 Effect of Test Variables

The initial condition of the test section, i.e., the moisture content or degree of saturation of the concrete material prior to testing, has a significant effect on the test results obtained during an FPT run. Generally, a higher flow rate of water into the concrete mass is obtained when the material is dry. More consistent and uniform results are obtained when the concrete is partially or fully saturated. Therefore, a vacuum pre-conditioning and subsequent pre-saturation of the test section prior to testing is recommended in case the concrete to be tested is relatively dry. The recommended test procedure is to allow the water to flow into the concrete for approximately 30 minutes, and then to begin regular flow measurements.

It has been established that test variables such as test orientation, partially filled test section, and removal of the test device between sequential or repetitive test runs should not have any significant effect on the final flow measurements obtained during an FPT.

CHAPTER 5  
TESTING AND EVALUATION OF IN-SERVICE MARINE STRUCTURES

5.1 Selected Concrete Bridge Structures

In-service marine concrete structures, mainly bridges that are located at or near the coastal regions of Florida, are classified as being exposed to extremely aggressive or highly corrosive environments and thus were targeted for testing for a "worst case scenario". The selection of these structures was primarily based on current needs and accessibility of the test site. An attempt was made to test a variety of bridge types ranging from high profile monumental bridge structures to small highway bridges. This offered the opportunity of testing and evaluating concrete bridge structures having different age, design, function, materials, and construction. Based on the scope and objectives set forth in this research study, and within the time and budget constraints, the following thirteen concrete bridge structures were selected and tested:

- (1) Seven-Mile Bridge, Florida Keys
- (2) Long Key Bridge, Florida Keys
- (3) Bahia Honda-Southbound Bridge, Florida Keys
- (4) Bahia Honda-Northbound Bridge, Florida Keys
- (5) Spanish Harbor Bridge, Florida Keys
- (6) Niles Channel Bridge, Florida Keys
- (7) Niles Channel Old Bridge, Florida Keys
- (8) B. B. McCormick Bridge, Jacksonville, Florida

- (9) SR-206 Bridge, Crescent Beach, Florida
- (10) Seabreeze Causeway Bridge, Daytona, Florida
- (11) Broward River (SR-105) Bridge, Jacksonville, Florida
- (12) Horse Creek Bridge, Melbourne, Florida
- (13) Horse Creek Old Bridge, Melbourne, Florida

Six of these bridge structures are located at the Florida Atlantic Intra-coastal Waterway (FAIW) while the other seven bridges are located at the Florida Keys region as indicated in the above list. The substructures of the above bridges, with the exception of Spanish Harbor Bridge, are shown in Figures 5.1 through 5.10. The majority of these bridges were designed for a service life of 50 years while the Seven-Mile and the Long Key bridges were designed for 75 years. The Seven-Mile Bridge was completed in October, 1982 after three years of construction at a total cost of \$45,820,469. As can be seen from Figure 5.1, this is a box-girder type, multiple span, high profile, monumental bridge structure spanning a total of seven miles over deep ocean waters. It is interesting to note that the same amount of time of construction was required to complete the much shorter bridge structure of Long Key in October, 1982 at a total cost of \$15,097,276. This also is a high profile, box-girder type bridge, but its substructure design is characterized by its V-shaped piers. A structure which has the same design as the Seven-Mile Bridge, but is of much smaller scale, is the Niles Channel Bridge which was completed within two years in April, 1983 at a total cost of \$8,948,575. This is the youngest structure of the concrete bridges selected for testing and evaluation in this study.

A concrete class IV specified to have a maximum allowable water/cement ratio of 0.41, and epoxy-coated reinforcing steel bars were used in the construction of the Seven-Mile, Long Key, and Niles Channel bridges. Cathodic protection (CP) systems have been installed on a total of 20 pile



Figure 5.1 Picture Showing the Substructure of the Seven Mile Bridge



Figure 5.2 Picture Showing the Substructure of Long Key Bridge



Figure 5.3 Picture Showing the Substructure of Bahia Honda Southbound (Right) and Northbound (Left) Bridges



Figure 5.4 Picture Showing the Substructure of Niles Channel Old (Right) and New (Left) Bridges



Figure 5.5 Picture Showing the Substructure of B. B. McCormick Bridge



Figure 5.6 Picture Showing the Substructure of SR-206 Bridge



Figure 5.7 Picture Showing the Substructure of Seabreeze Causeway Bridge



Figure 5.8 Picture Showing the Substructure of the Broward River Bridge



Figure 5.9 Picture Showing the Substructure of Horse Creek Bridge

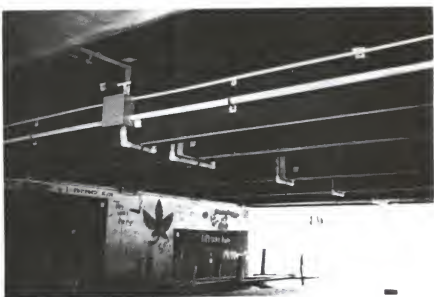


Figure 5.10 Picture Showing the Substructure of the Old Horse Creek Bridge

columns of the B. B. McCormick Bridge, and on the east-end pile caps (footers) of the SR-206 bridge. Conductive coating has been applied to 60 piles and conductive concrete applied to 10 piles of the Seabreeze Causeway Bridge while conductive coating has been applied to the underdecking beams and end-walls of the Horse Creek Bridge and to approximately 45 piles of the Broward River Bridge.

The installation of these CP systems, with the exception of that installed on the Broward River Bridge, was a part of a demonstration project partially funded by the FHWA at a total budget of about \$175,000. Once the project began, it was found that most of the piling of the Seabreeze Causeway Bridge required considerable repairs of spalled concrete. Installation of conduit and wiring proved to be extremely labor intensive and required a multitude of support services and equipment to access the higher elevations of the bridge. From the monitoring and evaluation that followed, it was concluded that the impressed current CP system using conductive mastic or conductive concrete was effective only in areas of the substructure that were not located near or within the tidal zone due to the fact that chloride accumulation and crystallization at the concrete-coating interface in this zone significantly increased the resistance in the circuit thereby restricting the current flow which in turn reduced the effectiveness of the system. Total disbondment of the protective coating occurred in several cases resulting in loss of the system. As the lower portion of the coated area became saturated with seawater due to either splash or abnormally high tide levels, a higher current density at the base (over protection) and a loss of cathodic protection potentials in the upper areas of the coated surfaces took place. On the other hand, conductive materials had to be placed as close to the high tide level as

possible in order to provide protection current to the steel reinforcement below the water level during the tide cycle. The precast panels at Horse Creek Bridge experience a tidal change of less than one foot. This offered a more favorable condition and less severe current distribution problem due to the fact that the concrete surface between the coating and the low tide level remained wet. The Seabreeze Causeway Bridge is subjected to a tidal variation of about 2.5 to 3 feet. The piles are exposed to almost constant wind and direct sunlight. This condition permits the area on the pile between the conductive concrete jacket and the receding water level to become dry. As this occurs, the resulting decrease in electrical conductivity significantly diminishes the ability to provide cathodic protection to the steel in the dryer area as well as the area below the water level. Although disbondment of the conductive concrete on piling at the Seabreeze Bridge was not observed, this system experienced the same current distribution problems as the conductive coating.

Figures 5.11 through 5.17 are pictures showing the extent and severity of concrete deterioration of the in-service concrete bridge structures selected for testing and evaluation in this study. Figures 5.11 through 5.13 are pictures of deteriorated piles of the Broward River Bridge substructure located at the FAIW in Jacksonville, Florida. It is interesting to note that, although these structural elements have been exposed to the same environmental conditions (chemical and physical) for years, they have exhibited several types of concrete deterioration with different patterns of distress. Excessive carbonation and general decomposition of the concrete material are the main causes of the concrete deterioration shown in Figure 5.11. Physical abrasion due to wave action may have contributed to some extent to the concrete deterioration which is demonstrated in this



Figure 5.11 Picture Showing Concrete Deterioration in a Pile (Broward River Bridge, Jacksonville)



Figure 5.12 Picture Showing Concrete Cracking due to Steel Corrosion in a Previously Repaired (Patched) Pile (Broward River Bridge, Jacksonville)



Figure 5.13 Picture Showing Extensive Vertical Cracking due to Steel Corrosion in a Pile (Broward River Bridge, Jacksonville)



Figure 5.14 Picture Showing Cracking of Concrete and Visible Corrosion Products in a Pile  
(B. B. McCormick Bridge, Jacksonville)



Figure 5.15 Picture Showing Excessive Vertical Cracking and Spalling of Concrete in a Pile (B. B. McCormick Bridge, Jacksonville)



Figure 5.16 Picture Showing Visible Steel Corrosion and Spalling of Concrete Cover in a Pile Cap (Seven-Mile Bridge, Florida Keys)



Figure 5.17 Picture Showing Excessive Steel Corrosion and Extensive Concrete Spalling in a Pier (Seven-Mile Bridge, Florida Keys)

case by the typical "hourglass" shape of the pile at the mean water level in the tidal zone. Concrete cracking due to corrosion of the embedded steel reinforcement and subsequent spalling of concrete cover is another type of concrete deterioration which is shown in Figure 5.12. Although the pile shown in this figure was previously repaired (patched), cracking and spalling of concrete cover continue to be the problem possibly due to inadequate treatment of an internally active corrosion region. Figure 5.13 shows extensive vertical cracking of concrete due to steel corrosion. This is a different pattern of concrete distress which is usually demonstrated in the form of continuous vertical cracking running parallel to and a few inches from the edge of the pile and extending several feet above the high-tide level into the splash zone (also see Figure 5.15). The tidal zone, defined as the region between the low and high-tide levels, is easily identified by the existence of various formations of marine organisms extending up to the high-tide level above which the splash zone begins.

Figures 5.14 and 5.15 are pictures of severely deteriorated piles of the B. B. McCormick Bridge substructure also located at the FAIW in Jacksonville, Florida. The type of concrete deterioration encountered in these structural elements is the same as the one demonstrated in Figure 5.13. However, the extent of deterioration is much more severe in this case, and corrosion of the embedded steel reinforcement is at an advanced state. Figure 5.14 depicts the formation of corrosion products that percolated through vertical cracks to the surface of the concrete and which are visible by the naked eyes. At such an advanced state, these corrosion products exert large tensile forces which cause more cracking and subsequent spalling of the concrete cover as shown in Figure 5.15. It should

be noted that the steel reinforcement in the concrete pile shown in this figure could readily be seen through the gap created in the material due to localized loss of concrete cover.

The extent and severity of concrete deterioration of in-service bridge structures in Florida are dramatically manifested in Figures 5.16 and 5.17. These are pictures of massive structural elements of the Seven-Mile Bridge substructure located in the Florida Keys region which is considered to be an extremely aggressive (highly corrosive) environment. Corrosion of the embedded steel reinforcement in this case is at the most advanced state where decomposition of the material and disbondment from the surrounding concrete is accompanied by a complete loss of concrete cover which, in turn, can lead to severe structural damage. Figure 5.16 is a picture showing the leaching of corrosion products and loss of concrete cover in a pier/pile cap. Figure 5.17 also demonstrates this type and degree of concrete deterioration which, in this particular pier, extends over an area of approximately 15 square feet of concrete and up to a height of about 9 feet above the tidal zone. This is contrary to the general belief that the most severe deterioration is likely to take place in the tidal zone because there the concrete is exposed to all kinds of physical and chemical attacks. As demonstrated in Figures 5.11 through 5.17, concrete deterioration due to corrosion or other chemical and physical attacks is not a phenomenon which is only encountered in the tidal zone and can readily be repaired or treated locally but is a more extensive problem with a potential of causing severe structural damage.

## 5.2 Field Testing Program

### 5.2.1 Field Operations

The field operations were arranged according to the FDOT field testing schedule, and performed in cooperation with the Corrosion Research Laboratory personnel of the Materials Office which provided the necessary assistance, equipment, and safety measures as needed. In situ permeability tests were performed on the selected concrete bridges using the developed FPT apparatus. FPTs were performed on structural elements such as partially submerged piling, pile columns, piers, pile caps, footers, bascules, etc., at various locations, elevations, and orientations. The majority of the structural elements tested were part of the substructure of these concrete bridges and they were only accessible by water. Therefore, the flow measurements for the in situ permeability tests were remotely taken by means of the FPT instrumentation unit which was carried on and operated from a boat. The rest of the field operations were performed from a specially designed work boat, provided and operated by the FDOT field crew, which was appropriately equipped to carry out such operations. For each FPT installation the following field operations were performed:

- (1) Site selection: the selection of the test site and structural element to be tested was primarily based on current needs, condition of the site concrete as determined from previous field inspection and evaluation data, and accessibility of test location.
- (2) Preparation of test location: in case the test location on the selected structural element was within the tidal or splash zones the concrete surface was cleaned from any marine organisms or other surface irregularities as shown in Figure 5.18. The test location was

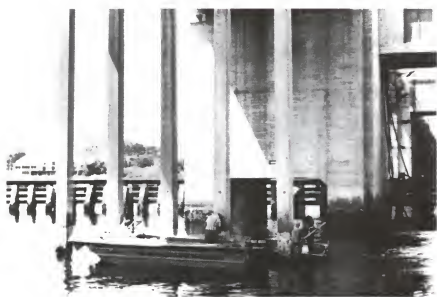


Figure 5.18 Picture Showing the Preparation of a Test Location

then appropriately marked for subsequent testing and recorded on the FPT data sheet.

- (3) Location of rebars: a standard portable rebar-locator device was used to determine the clear concrete cover and the size and location of the steel reinforcement with respect to the selected test location. This operation was important in order to avoid causing any damage to the drilling equipment, altering the structural integrity of the tested concrete element, and ensuring that no discontinuity was present in the FPT flow region.
- (4) Coring of test holes: the 7/8-inch diameter, 6-inch deep test holes were drilled at the selected test locations by means of a portable core drilling rig utilizing a diamond-dressed core bit and a continuous supply of pressurized water. The drilling rig could readily be fastened perpendicularly on the concrete surface thus allowing the drilling of a test hole at any orientation and elevation as shown in Figure 5.19.
- (5) Extraction of cored samples: samples of the site concrete tested with the FPT apparatus were obtained using the above-mentioned coring equipment in order to be used in the laboratory for further testing and evaluation of the concrete material. Concrete cores, 1.75 inches in actual diameter and minimum 3 inches in length, were extracted from locations on structural elements which were as close as possible to the test sections tested by the FPT in order to obtain comparative samples of the concrete material. In case slender structural elements, as the one shown in Figure 5.20, were tested the maximum distance of a cored sample from the FPT hole was 12



Figure 5.19 Picture Showing the Coring of a Test Hole



Figure 5.20 Picture Showing the Location of Extracted Cored Concrete Sample with Respect to the Test Hole

inches. From massive structural elements such as bascules, concrete cores of up to 8 inches in height were extracted from locations within 6 inches from the FPT hole. These cored concrete samples were further prepared in the laboratory and used for the determination of chloride-ion permeability of concrete according to the standard method AASHTO T277-83 previously described in Section 2.4.

(6) Determination of moisture content: the moisture content of the in situ concrete was determined before any actual testing was performed by means of a portable (battery operated), nondestructive moisture meter. The device used was entirely electronic with a digital display, utilizing the latest silicon chip technology to measure the quantity of water within its electromagnetic field extending several inches deep into the concrete material. This particular moisture meter was calibrated by the manufacturer to indicate the relative moisture content in percentage, ranging from 0% to 20%, with the lower limit indicating an oven-dry condition and the upper limit corresponding to a fully saturated (100%) condition. Since no precision statement was provided by the manufacturer and the accuracy of this meter could not readily be established, this device was used for the measure of relative in situ moisture and only for comparative purposes. In case the meter indicated that the in situ concrete was relatively dry, a vacuum pre-conditioning and subsequent pre-saturation of the test section prior to testing were applied as described in Section 3.7 and in Appendix A. Relative moisture readings at the four diagonal points around the test hole were taken, as shown in Figure 5.21, before and after each FPT run, and recorded along with the average value on the FPT data sheet.



Figure 5.21 Picture Showing the Measurement of In Situ Moisture Content of Concrete

- (7) Performance of FPTs: FPTs were performed on the selected concrete bridges at the prepared test locations according to the testing and operating procedures described in Section 3.7 and in Appendix A. Retesting of the same test hole was applied in case this was deemed essential in clearly establishing the reliability of the obtained test results. Therefore, repetitive FPT runs were performed in a number of field installations.
- (8) Patching of concrete holes: patching of the FPT holes as well as the 1.75-inch-diameter cored holes was applied immediately following the completion of all the necessary testing on the selected structural elements. An appropriate mix of sand, cement, water and, in some cases, fast-curing epoxy was applied in the holes and the surface of the concrete was properly finished.

#### 5.2.2 Field Permeability Test Results

The FPT measurements obtained from the above field testing operations performed on the selected concrete bridges were analyzed according to the procedure described in Section 3.8. The coefficient of permeability of concrete was determined for each test section tested by means of Equation 3.10A. The FPT results, along with all other pertinent data obtained from the field, are summarized in Table 5.1.

Some difficulty was encountered in determining the relative moisture content of the in situ concrete under the existing site conditions. It appeared that ambient conditions such as temperature and humidity as well as surface irregularities of the tested concrete had a significant effect on the moisture measurements at each point, as manifested by the high fluctuations in the readings displayed by the moisture meter used. Although the readings obtained with this device should be interpreted with

Table 5.1 Summary of Results Obtained from FPTs Performed on In-Service Concrete Bridge Structures

CONCRETE BRIDGE STRUCTURE TESTED	TYPE OF STR. ELEMENT TESTED	TEST LOCATION	TEST PRESSURE (psi)	PERMEABILITY COEFFICIENT ( $\times 10^{-9}$ cm/sec)	% AVG. RELATIVE MOISTURE CONTENT OF CONCRETE BEFORE TEST / AFTER TEST
SEVEN MILE	PIER STRUT	#1, 14 S-A	200	1.90	13.84
	"	#1, (R)	200	1.85	13.66
	"	#2, 13 TOP	200	6.69	11.08
	"	#2, (R)	200	8.09	11.60
LONG KEY	V-PIER CAP	#1, 103 TOP	500	0.94	(N/A)
	"	#2, 96 TOP	500	2.47	(N/A)
	"	#3, 66 TOP	500	2.36	(N/A)
	FOOTER CAP	#1, TOP-W	200	7.21	11.31
BAHIA HONDA - SOUTHBOUND	"	#2, TOP-W (*C)	200	27.76	10.25
	"	#3, TOP-E	200	6.65	11.44
	"	#4, TOP-E (*C)	200	42.12	11.75
	"	#1, TOP-E	200	5.25	11.25
BAHIA HONDA - NORTHBOUND	"	#1, (R)	200	6.21	12.53
	"	#2, TOP-E	200	23.93	12.36
	"	#3, TOP-W	200	37.25	13.10
	PILE COLUMN	#1, 7 S-A	200	3.81	16.60
SPANISH HARBOR	"	#2, 6 S-A	200	2.88	15.17
	"				16.18

Table 5.1--continued.

CONCRETE BRIDGE STRUCTURE TESTED	TYPE OF STR. ELEMENT TESTED	TEST LOCATION	TEST PRESSURE (psi)	PERMEABILITY COEFFICIENT (x10 <sup>-9</sup> cm/sec)	% AVG. RELATIVE MOISTURE CONTENT OF CONCRETE BEFORE TEST / AFTER TEST
SPANISH HARBOR	PILE COLUMN	#3, 7 S-A	200	3.96	16.56
	"	#4, 6 S-A	200	4.38	15.27
NILES CHANNEL	PIER FOOTER	#1, 9 W-A	200	1.46	15.91
	"	#2, 6 N-A	200	1.78	12.80
NILES CHANNEL - OLD	PIER STRUT	#1, 9 W-A (*C)	200	14.70	14.78
	ARCH WALL	#1, 9 W-B (*C)	200	51.03	13.81
B. B. MCGORMICK	"	#2, 6 W-B (*C)	200	66.55	14.38
	PILE COLUMN	#1, 1 E-A (*C)	500	10.00	9.90
	"	#1, (R)	500	9.50	12.00
	"	#2, 1 W-A	250	45.70	5.84
	"	#2, (R)	250	38.90	9.28
	"	#2, (R)	250	35.60	9.79
	"	#3, 2 S-A	250	47.20	8.40
	PILE COLUMN	#3, (R)	250	45.20	9.62
ONSHORE PIER	"	#4, 3 S-A	250	14.50	6.44
	"	#1, 3 S	500	19.80	10.90
					13.31

Table 5.1--continued.

CONCRETE BRIDGE STRUCTURE TESTED	TYPE OF STR. ELEMENT TESTED	TEST LOCATION (*C)	TEST PRESSURE (psi)	PERMEABILITY COEFFICIENT (x10 <sup>-9</sup> cm/sec)	% AVG. RELATIVE MOISTURE CONTENT OF CONCRETE BEFORE TEST / AFTER TEST
B. B. McCORMICK	ONSHORE PIER	#2, 3 S (*C)	500	8.10	12.55
	"	#3, 3 S	500	41.70	8.35
	"	#3, (R)	500	36.70	9.56
	"	#3, (R)	500	34.80	10.70
	"	#4, 4 W	275	22.80	10.56
	"	#4, (R)	300	24.01	10.89
	GIRDER	#1, TOP	300	12.00	4.01
SR206-CRESSENT BEACH	"	#2, E	300	1.53	12.74
	"	#3, E	300	5.65	10.20
	PILE	#4, S	300	6.26	9.07
SEABREEZE CAUSEWAY	WEST BASCULE	#1, S-B	200	25.80	14.36
	"	#1, (R)	200	20.80	16.31
	"	#2, S-A (*C)	200	11.10	14.41
	EAST BASCULE	#1, N-B (*C)	200	24.60	14.52
	"	#1, (R)	200	20.10	15.98
	"	#1, (R)	200	19.20	13.83
					17.03

Table 5.1-continued.

CONCRETE BRIDGE STRUCTURE TESTED	TYPE OF STR. ELEMENT TESTED	TEST LOCATION (*C)	TEST PRESSURE (psi)	PERMEABILITY COEFFICIENT (x10 <sup>-9</sup> cm/sec)	% AVG. RELATIVE MOISTURE CONTENT OF CONCRETE BEFORE TEST / AFTER TEST
BROWARD RIVER	BASCULE	#1, W-A	200	6.08	5.72
	PILE	#1, E-A	200	8.03	12.76
	"	#2, E-B	200	32.50	4.83
HORSE CREEK	BEAM	#1, S	300	10.64	14.82
	"	#2, S	300	7.97	10.37
	"	#3, S	200	11.12	12.76
HORSE CREEK - OLD	END WALL	#1, S (*C)	300	5.91	11.76
	"	#2, S (*C)	200	6.73	11.64
					13.87

Key:  
 A = Above high-tide level i.e., Splash Zone  
 B = Below high-tide level i.e., Tidal Zone

E = East face

W = West face

N = North face

S = South face

(\*C) = Indicates 1.75-inch diameter core sample extracted from concrete

(R) = Indicates re-testing of test section  
 (N/A) = Data not available

caution, the average measurements of the relative moisture content of the in situ concrete showed a definite increase in water content during each test run, as demonstrated by the data in Table 5.1, indicating that the developed FPT probe was able to properly inject water radially into the surrounding concrete mass.

Repetitive FPTs performed at the same test section on different types of structural elements produced permeability coefficients having maximum percent difference ranging from about 3% to 28%, as the data in Table 5.2 show. The results obtained from these replicate tests indicated that the FPT method demonstrated acceptable repeatability under actual field conditions. However, very high discrepancies were observed between the mean coefficients of permeability obtained from FPTs performed at different test locations on structural elements having the same design and/or concrete type. As can be seen from Table 5.3, the maximum percent difference in such cases ranged between about 5% to 684%. It is interesting to note that the highest variation among permeability coefficients of same class concrete was obtained from FPTs performed at three different test sections on a girder at SR206 - Crescent Beach bridge which was built in 1975. From the total of 57 individual FPTs run on the 13 selected concrete bridges, the lowest registered value of permeability coefficient, 0.1I-9 cm/sec, was the one obtained from a test section on a V-pier cap of Pier #103 at the Long Key bridge. Overall, the permeability coefficients of the tested site concretes were, on the average, two to four orders of magnitude higher than the coefficients obtained from FPTs performed on laboratory prepared concretes of similar quality. These results are further discussed in Section 5.5.

Table 5.2 Repeatability of FPTs Performed at the Same Test Section

CONCRETE BRIDGE STRUCTURE TESTED	TYPE OF STRUCTURAL ELEMENT	PERMEABILITY COEFFICIENT ( $\times 10^{-9}$ cm/sec)		MAXIMUM PERCENT DIFFERENCE
		1st TEST	RE-TEST	
SEVEN MILE	PIER STRUT	1.90	1.85	2.70
	"	6.69	8.09	-17.30
BAHIA HONDA - N	FOOTER CAP	5.25	6.21	-15.46
B. B. McCORMICK	PILE COLUMN	10.00	9.50	5.26
	"	45.70	35.60	28.37
	"	47.20	45.20	4.43
	ONSHORE PIER	41.70	34.80	19.83
		22.80	24.01	-5.04
SEABREEZE CAUSEWAY	BASCULE	25.80	20.80	24.04
	"	24.60	19.20	28.12

Table 5.3 Comparison of Results Obtained from FPTs Performed on Structural Elements of Same Type and Concrete Material

CONCRETE BRIDGE STRUCTURE TESTED	TYPE OF ELEMENT TESTED	TEST SECTION	MEAN COEFFICIENT OF PERMEABILITY ( $\times 10^{-9}$ cm/sec)	MAXIMUM PERCENT DIFFERENCE
SEVEN MILE	STRUT	1	1.875	294.13
	"	2	7.390	
LONG KEY	PIER CAP	1	3.880	162.77
	"	2	2.470	
	"	3	2.360	
BAHIA HONDA - SOUTHBOUND	FOOTER	1	7.210	533.38
	"	2	27.760	
	"	3	6.650	
	"	7	42.120	
BAHIA HONDA - NORTHBOUND	"	1	5.730	550.09
	"	2	23.930	
	"	3	37.250	
SPANISH HARBOR	PILE	1	3.880	6.89
	"	2	3.880	
NILES CHANNEL	FOOTER	1	1.780	21.92
	"	2	1.780	
NILES CHANNEL - OLD	WALL	1	51.030	30.41
	"	2	66.550	
B. B. McCORMICK	PILE	1	9.750	470.37
	"	2	40.070	
	"	3	46.200	
	"	4	14.500	
	"	5	19.800	
	"	6	3.700	
	"	7	37.730	
	"	8	23.400	

Table 5.3--continued.

CONCRETE BRIDGE STRUCTURE TESTED	TYPE OF ELEMENT TESTED	TEST SECTION	MEAN COEFFICIENT OF PERMEABILITY ( $\times 10^{-9}$ cm/sec)	MAXIMUM PERCENT DIFFERENCE
SR206 - CRESCENT BEACH	GIRDER	1	12.000	684.31
	"	2	1.530	
	"	3	5.650	
SEABREEZE CAUSEWAY	BASCULE	1	23.300	109.91
	"	2	11.100	
	"	3	21.300	
BROWARD RIVER	PILE	1	8.030	304.73
	"	2	32.500	
HORSE CREEK	BEAM	1	10.640	4.51
	"	2	7.970	
	"	3	11.120	
HORSE CREEK - OLD	WALL	1	5.910	13.87
	"	2	8.030	

### 5.3 Laboratory Testing Program

#### 5.3.1 Modification of the Chloride Permeability Test

The standard method of test for rapid determination of the chloride permeability of concrete, AASHTO T277-83, previously reviewed in Section 2.4, was employed in this study in order to further evaluate the concrete material of the in-service bridge structures under investigation. Cored concrete samples were obtained from the field according to the procedure described in step (5) in Section 5.2.1. The test locations these cores were extracted from are indicated in Table 5.1. Figure 5.22 is a picture showing an actual concrete core obtained from one of these test locations, and a prepared specimen as used in the chloride test. Since the 1.75-inch actual diameter of these cores was smaller than the standard 3.75-inch diameter normally used in this test, the dimensions of the inside diameter of the applied voltage cell were modified to fit the outside diameter of the prepared field specimens. Figure 5.23 is a picture showing the modified applied voltage cell fabricated for this study according to the construction specifications provided in the AASHTO method as well as in Reference 20.

During the preliminary testing of some of the cores using the modified applied voltage cell, high temperatures were observed usually within the first two hours of test duration. An additional modification was applied to the chloride test since temperatures as high as 180F were registered resulting in the damage of the cell after repeated test runs. Therefore, the level of applied voltage was reduced from the standard 60 volts to 30 volts in order to avoid equipment failure due to the observed higher current flows through the tested concrete samples.



Figure 5.22 Picture Showing a Field Concrete Core (Right) and a Prepared Specimen (Left)

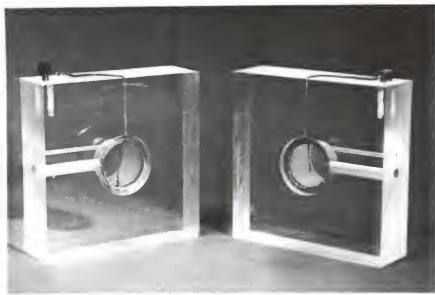


Figure 5.23 Picture Showing the Modified Applied Voltage Cell

Due to the above modifications, the results obtained from the rapid chloride permeability test were adjusted accordingly to take into account the reduced cross-sectional area of the concrete specimens and the reduced applied voltage. The test measurements were normalized to correspond to standard results by applying an adjustment factor,  $C_a$ , determined as follows:

The electrical resistivity,  $\rho$ , of any material is defined as the resistance between opposite faces of a unit specimen of the material according to the following equation:

$$\rho = R A / L \quad (5.1)$$

where

$R$  = electrical resistance of specimen

$A$  = cross-sectional area of specimen

$L$  = length of specimen

According to Ohm's law,

$$I = V / R \quad (5.2)$$

where

$I$  = electrical current

$V$  = applied voltage

Since the length of the concrete specimens used in the chloride test device was constant (2 inches) and the resistivity of the concrete material during the testing was assumed to remain constant, the relationship between the standardized and modified chloride test results can be represented by the following equation:

$$I_{60} / I_{30} = V_{60} A_{60} / V_{30} A_{30} = C_a \quad (5.3)$$

where

$I_{60}$ ,  $V_{60}$ ,  $A_{60}$  = Test parameters at the standard 60 volts level

$I_{30}$ ,  $V_{30}$ ,  $A_{30}$  = Test parameters at the reduced 30 volts level

Substituting the appropriate values in Eqn. 5.3, we get  $C_a = 9.18$  which is the adjustment factor which was applied to normalize the test results obtained by the modified chloride test to correspond directly to the standard chloride permeability results (coulombs) as interpreted in the AASHTO T277-83 method.

### 5.3.2 Chloride Permeability Test Results

Rapid chloride permeability tests were performed in the laboratory on a number of cored concrete specimens obtained from the selected bridge structures under investigation. The concrete cores used in this series of tests were obtained from structural elements which had already been tested for their relative water permeability by means of the developed FPT apparatus. These cores were extracted from each concrete element according to the procedure described in step (5) in Section 5.2.1, and from locations which are indicated in Table 5.1.

The field cored concrete specimens were sectioned in 2-inch slices, and subsequently conditioned and prepared for testing according to the procedure stipulated by the AASHTO T277-83 method. As many as three 2-inch slices were cut from the top (A), middle (B), and bottom (C) sections of long field cores when possible. The middle (B) section of shorter concrete cores, corresponding to the region of concrete material tested with the FPT, was used in these tests for comparative purposes. The test measurements were analyzed according to the standard procedure, and the adjustment factor  $C_a$  was applied to convert the chloride permeability results

(coulombs) to correspond to standard values. The results from this series of laboratory chloride permeability tests are presented in Table 5.4.

The maximum percent difference between the values of charge passed (coulombs) of test specimens taken from the top, middle, and bottom sections of field concrete cores ranged between about 1% to 242%. A relatively high variation was also observed among the values of structural elements having the same design and/or concrete class as in the case of the water permeability results. A closer examination of the experimental results of the rapid chloride permeability tests reveals an interesting trend in the coulomb values obtained from different sections of the same concrete cores. In 80% of the cases, the total electrical charge (coulombs) which passed through the tested concrete material during the duration of each chloride test was higher for concrete specimens cut from the bottom (C) or the middle (B) sections of cores as compared with those cut from the top (A). This trend along with the discrepancies in the test results obtained for the same class concretes indicated a significant variation in the quality and durability characteristics as reflected by the obtained chloride and water permeability values of the tested concretes. The interpretation of all of the above permeability test results are further discussed in Section 5.5.

#### 5.4 Correlation Between the Results of the Developed FPT Method and the AASHTO T277-83 Method

The results obtained from the developed FPT method, presented in Table 5.1, and the standard AASHTO T277-83 method, presented in Table 5.4, were compared in order to determine whether there was any relation between the water permeability and the charge passed through the tested concretes.

Table 5.4 Results of the Rapid Chloride Permeability Tests

CONCRETE BRIDGE	TYPE OF ELEMENT	SPECIMEN No.	CHARGE PASSED (COULOMBS)	MAX. % DIFFERENCE
SEABREEZE CAUSEWAY	BASCULE	1B	3,857.4	N/A
		2B	7,547.9	N/A
B. B. McCORMICK	PILE	3B	3,422.3	N/A
	PIER	4B	2,658.9	N/A
BROWARD	BASCULE	5B	1,921.7	N/A
OLD HORSE CREEK	WALL	6A	2,111.8	0.76
	"	6B	2,127.9	
	"	7A	3,158.2	N/A
	"	8B	1,937.8	127.45
	"	8C	4,407.5	
NEW HORSE CREEK	BEAM	9A	2,735.3	178.68
		9B	5,252.2	
		9C	7,622.7	
	10B		2,311.0	242.02
	10B		7,904.1	
NILES CHANNEL	STRUT	11A	5,855.6	35.02
	"	11B	7,906.2	
OLD NILES CHANNEL	WALL	12A	18,368.1	21.22
	"	10B	15,153.1	
	"	13B	18,227.6	N/A
SP. HARBOR	PILE	15A	10,457.5	N/A
BAHIA HONDA SOUTH BOUND	FOOTER	10B	9,205.7	9.79
	"	16C	10,107.2	
	"	17B	11,390.0	
	"	17C	7,757.5	46.83

Table 5.4--continued.

CONCRETE BRIDGE	TYPE OF ELEMENT	SPECIMEN No.	CHARGE PASSED (COULOMBS)	MAX. % DIFFERENCE
BAHIA HONDA NORTH BOUND	FOOTER	18B	7,758.6	46.29
	"	18C	11,350.1	
	"	19A	7,926.2	26.22
	"	19B	10,004.4	

Key: N/A = Not Applicable

Note: According to the standard AASHTO T277-83 method:

<u>Charge Passed (coulombs)</u>	<u>Chloride Permeability</u>
>4,000	High
2,000-4,000	Moderate
1,000-2,000	Low
100-1,000	Very Low
<100	Negligible

Since in an FPT, the center of the flow region in the test hole was located 3 inches from the surface of the concrete, the chloride permeability test results obtained from the specimens cut from the middle of concrete cores (B-series) which corresponded to the FPT section were used for comparison. The respective permeability test results are presented in Table 5.5.

A correlation analysis of these values was performed using linear regression. The results of the regression analysis were as follows:

$$Q_{RCP} = 247.7167 K_{FPT} + 1834.190 \quad (5.4)$$

$$R^2 = 0.9000454$$

$$\text{Number of Observations} = 16$$

$$\text{Standard Error of the Slope} = 22.012540$$

where

$Q_{RCP}$  = Charge passed (coulombs) measured by the Rapid Chloride Permeability (RCP) Test Method

Figure 5.24, which is a graphical representation of the above results, suggests that it is possible to assume a linear relationship between the respective chloride and water permeability values as determined by the two methods. Although limited experimental values were considered in this analysis, the obtained coefficient of determination ( $R^2$ ) of 0.90 indicates a strong relation between the two quantities.

### 5.5 Evaluation of the Tested Site Concrete

The evaluation of the in-service concrete structures investigated in this study was performed from the concrete material point of view and with respect to the physical property of permeability. Although in many cases, the deterioration of concrete material and the other related durability

Table 5.5 Comparison of Results Obtained from the FPT and Rapid Chloride Permeability Test

CONCRETE BRIDGE STRUCTURE TESTED	TYPE OF STRUCTURAL ELEMENT	CHLORIDE PERMEABILITY B-SERIES (COULOMBS)	MEAN WATER PERMEABILITY COEFFICIENT (xE-9 cm/sec)
SEABREEZE CAUSEWAY	BASCULE	3,857.4	14.70
	"	7,547.9	21.30
B. B. McCORMICK	PILE	3,422.3	9.75
	PIER	2,658.9	8.10
BROWARD RIVER	BASCULE	1,921.7	6.08
HORSE CREEK - OLD	WALL	2,127.9	5.91
	"	1,937.8	6.73
HORSE CREEK - NEW	BEAM	5,252.2	10.64
	"	7,904.1	7.97
NILES CHANNEL	STRUT	7,906.2	14.70
NILES CHANNEL - OLD	WALL	15,153.1	51.03
	"	18,227.6	66.55
BAHIA HONDA - SOUTHBOUND	PIER FOOTER	9,205.7	27.76
	"	11,390.0	42.12
BAHIA HONDA - NORTHBOUND	"	7,758.6	23.93
	"	10,004.4	37.25

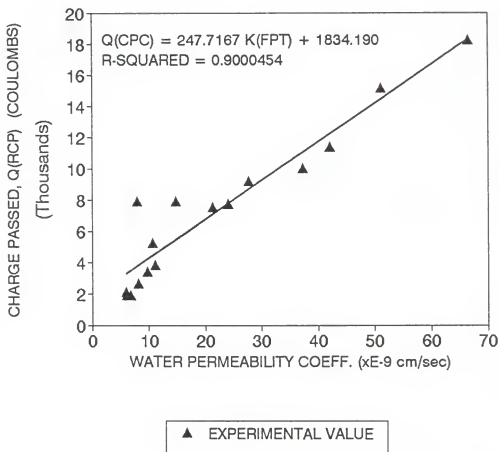


Figure 5.24 Correlation Between Charge Passed and Water Permeability Coefficient

problems would directly induce structural distress and local failure, structural evaluation of the tested in-service bridges was beyond the scope of this research. Instead, the tested concrete material of these bridges was evaluated for its relative performance and durability based on the obtained FPT and rapid chloride permeability test results. However, the information provided by the visual inspection of the structural elements of these bridges was taken into consideration in the evaluation process.

In order to properly assess the performance and durability of the tested concrete material in the selected in-service bridges, it was important to collect the appropriate information listed in Section 3.8.1 for each structure. Since the evaluation of concrete was performed from the material point of view, the most crucial data required for the proper assessment of the durability were the cement and aggregate types, the concrete class, and the related mix design parameters as specified and used in the construction of these concrete bridges. The collection of this pertinent information proved to be impossible due to the fact that no such data were readily available for bridge structures constructed prior to 1980. The majority of the marine structures under investigation were constructed in a much earlier period, and some of them as early as the beginning of the century, e.g., Old Niles Channel Bridge in the Florida Keys region. Therefore, limited material data were available for only the three bridge structures which were built after 1980 namely, the Seven Mile, the Long Key, and the (New) Niles Channel bridges. The FDOT Materials Office provided the following data for these three and few other concrete bridge structures:

- a) Concrete class IV having maximum allowable water/cement ratio of 0.41 was specified for the substructure. A target water/cement ratio of 0.35 was set for the concrete batches produced. The final water/cement ratio of the concrete usually placed on the structural elements of these bridges ranged between 0.37 to 0.39. Concrete class IV was also used at SR-206 Crescent Beach bridge which was constructed in 1975.
- b) Cement Types II, I & III, and II & III were specified and used at Seven Mile, Long Key, and Miles Channel bridges, respectively.
- c) The aggregate type for the concrete used at B. B. McCormick bridge, which was constructed in 1949, was a river gravel while porous limestone was used at all the other concrete bridge structures.

Comparison of the results obtained from FPTs performed on the selected in-service concrete structures with those obtained from water permeability tests on laboratory prepared concrete specimens of similar quality and materials indicates that the site concretes exhibited very high water permeabilities. Based on the analysis presented in Section 5.2.2, it could be inferred that the site concretes under evaluation exhibited poor durability characteristics and high variability in quality and performance as attested by the results of their relative water permeabilities.

According to the standard AASHTO T277-83 method, conventional portland cement concrete of low water/cement ratio (<0.4), which corresponds to the class IV concrete used in some of the above-mentioned bridge structures, is typically expected to have low chloride permeability corresponding to a total charge passed ranging between 1,000 to 2,000 coulombs as indicated in Table 5.4. However, only 6.90% of the tested concrete

specimens produced results which were within this range, while 27.59% and 65.52% of the specimens exhibited moderate and high chloride permeabilities, respectively. All of the concrete specimens extracted from bridge structures located in the Florida Keys region exhibited high chloride permeabilities. The highest registered charge passed through a tested concrete material, 18,368.1 coulombs, was obtained from a concrete core extracted from the arch wall of bent #9 at the Old Niles Channel bridge. This value was about 359% higher than the upper limit of charge passed corresponding to high chloride permeability according to the AASHTO T277-83 method. Based on the high quantities of charge passed through the majority of the tested concretes, and the observed high variation of values obtained from duplicate specimens tested with the rapid chloride permeability method, it could be inferred that there was a significant variation in the quality and durability characteristics of the concrete with respect to chloride permeability.

Although the site concrete at the particular locations where FPTs were performed and/or cored samples were extracted from was sound and did not exhibit any visual signs of deterioration, corrosion or other patterns of distress, the results obtained from the field and laboratory testing programs indicated poor durability characteristics with respect to permeability, and questionable level of quality with potential for future performance problems of the tested concrete material under the given exposure conditions. The obtained results further suggest that there seems to be an apparent relationship between the condition of structural concrete and its permeability. It is believed that the relatively high permeability of

the concrete significantly contributed to the deterioration of some elements at these bridge structures by allowing the intrusion of deleterious substances present in the marine environment into the concrete material.

CHAPTER 6  
RECOMMENDED TESTING AND EVALUATION SCHEME  
USING THE DEVELOPED FPT METHOD

6.1 Proposed Testing Scheme

Based on the findings of this research study, it can be concluded that the developed FPT apparatus and method appear promising in providing a suitable measuring system for rapid determination of the in situ permeability of structural concrete. It is believed that the developed experimental testing method could effectively be implemented and incorporated into a broader testing scheme in the future for the proper assessment of the quality, performance, and durability of concrete in marine structures.

The results obtained by the developed FPT method demonstrated strong positive correlation with those obtained by an existing laboratory permeability test set-up with known reliability. A good correlation was also demonstrated between the values of the coefficient of water permeability of concrete obtained from FPTs performed on marine structures and the results obtained from rapid chloride permeability tests performed on representative field cored concrete samples extracted from these structures according to the standard AASHTO T277-83 method. The empirical relationships obtained in this study indicated that the developed FPT method could be used in conjunction with these and other existing test methods or techniques for an effective evaluation of the performance and durability of concrete in marine structures. A proposed integrated testing scheme for this purpose is presented in Figure 6.1.

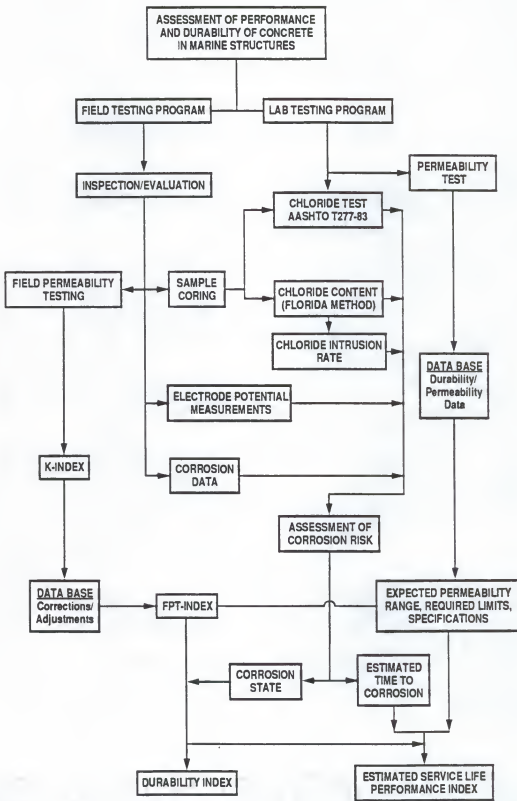


Figure 6.1 Proposed Testing Program for Marine Structures

The proposed testing scheme can be divided into two major parts namely, the field testing program and the laboratory testing program. The main characteristic of this testing scheme is that a number of operations within each testing program could be performed independently and at a different time while operations between each program could be performed concurrently. This drastically reduces the time and effort required to perform certain tasks and results in an efficient way of collecting and processing the experimental data.

Under the field testing program, in addition to the information furnished by the FPTs, other in situ data such as electrode potential measurements and corrosion data could be provided which would further be analyzed and evaluated under the laboratory testing program. Field cored concrete samples (1.75-inch-dia.) obtained from locations on bridge structures could be tested in the laboratory for their relative chloride permeability by means of the standard AASHTO T277-83 method while the small cores (0.726-inch-dia.) obtained from each FPT hole could be used to determine the chloride content of concrete by means of the Florida Method. The chloride content values could further be used in the determination of the average chloride intrusion rate which, in turn, could provide an estimate of the time to corrosion of rebars. In cases where 4-inch-diameter cores were permitted to be extracted from the structure, the existing laboratory permeability test set-up could be used to evaluate the specimens under long-term testing. Most importantly, the existing data base developed in a previous study employing the laboratory permeability test method could not only provide expected permeability values of the various concrete classes used in Florida but could also furnish valuable information on the effects of different curing conditions, water/cement ratio, cement type and admixtures, aggregate type used and other mix design parameters

on the permeability of structural concrete. These and other data on expected permeability ranges, required limits or specifications would be compared to the experimental data collected from the field and laboratory testing programs to determine whether acceptable results were obtained.

After incorporating all of the above data and results in the analysis process, the integrated testing scheme merges to the final evaluation stage which consists of the assessment of the corrosion risk and the determination of the durability and performance indices. In case the concrete structure under evaluation is relatively young or currently under construction, the estimated time to corrosion can be determined by means of the standard Test Method No. Calif. 532-A developed by the Materials and Research Department of the State of California, Department of Public Works, Division of Highways, which has previously been used by the FDOT and was proven to produce reliable estimates. For bridge structures which have been in service and have consequently been exposed to environmental conditions for some years, the state of corrosion can be determined by means of visual inspection and evaluation of the physical condition of the site concrete, field measurements of electrical potentials, depth of carbonation measurements, and other available corrosion evaluation techniques. Based on all of the above information, appropriate durability and performance indices could be assigned accordingly and the estimated service life of the structure be determined. A worked example demonstrating the application of the proposed testing scheme is presented in Appendix B.

#### 6.2 Recommended Permeability Ranges for the Developed FPT

The developed FPT apparatus and method were shown to give consistent and reliable test results (values of permeability) under both laboratory as well as actual field conditions. The apparent permeability coefficients

as determined by the FPT method could be taken as a measure of the relative performance and durability of the concrete in existing in-service concrete structures. The FPT results could provide valuable information on the quality of the concrete materials used in newly constructed as well as aged in-service bridge structures. The FPT measurements could also give an indication on the potential of the concrete material to provide the necessary protection to the embedded reinforcing steel against the intrusion of deleterious substances such as chloride ions which can cause corrosion and subsequent deterioration to the structure.

Based on the experimental values obtained in the laboratory and field testing programs conducted in this research study, the FPT results can be interpreted according to the recommended ranges presented in Table 6.1. It should be noted that the given tabulated values are not absolute since they are based on limited experimental field testing. Care should be taken in interpreting the values of this test since the initial moisture condition or degree of saturation of concrete has a significant effect on the obtained results. Although the pre-conditioning technique employed in the FPT procedure appears to offset the effect of in situ moisture content, no definite relationship has been established in this respect during the present study. However, it is believed that if the tested site concrete is partially submerged and has been exposed to tidal action for a period of years, a saturated condition is in place and thus the effect of moisture can be assumed to be minimal for all practical purposes. The developed FPT method should not be used as a substitute of other existing laboratory test methods for investigating the influence of various factors that affect the permeability of concrete. Rather, it is intended for use in the field as a rapid method for the determination of the in situ permeability of concrete. The FPT is recommended to be used

Table 6.1 Interpretation of FPT Results

FPT Coefficient Value (cm/sec)	Relative Permeability Ranking
$>2 \times 10^{-8}$	Very High
$5 \times 10^{-9} - 2 \times 10^{-8}$	High
$1 \times 10^{-11} - 5 \times 10^{-9}$	Moderate
$1 \times 10^{-12} - 1 \times 10^{-11}$	Low
$1 \times 10^{-13} - 1 \times 10^{-12}$	Very Low
$<1 \times 10^{-13}$	Negligible

in conjunction with other standardized tests for the relative measurement of permeability and as an indicator of the durability of concrete.

## CHAPTER 7 CONCLUSIONS AND RECOMMENDATIONS

### 7.1 Summary and Conclusions

The scope of this research study was the assessment of the performance and durability of the concrete material of existing in-service marine structures under actual field conditions with respect to permeability. At present, there does not exist any standard method for the direct determination of the in situ water permeability of structural concrete. There was a need to develop a test apparatus and method which would allow regular in situ permeability measurements, i.e., without the requirement to extract cored specimens from the concrete structure and test them in a laboratory permeability test apparatus.

In this study, an FPT apparatus and method was developed and evaluated in both the laboratory and in the field. The developed prototype FPT apparatus and method were used in the testing and evaluation of in-service marine structures. The developed FPT method was used in conjunction with other existing techniques and standard methods in a comparative study, and good correlation was demonstrated between the experimental results obtained by each method employed. Based on the experimental results obtained in the laboratory and field testing programs employed in this research study, recommended ranges of the permeability coefficient as determined by the FPT method were established for the assessment of the relative performance and durability of concrete in marine structures.

In the development of a portable, quasi nondestructive device to measure the in situ permeability of in-service concrete, several different designs were attempted, and a number of devices were constructed and evaluated until the current prototype was finally adopted. After months of experimentation, an effective design was achieved, and a suitable FPT apparatus, which satisfied all the design requirements set forth in this study, was fabricated. The developed FPT apparatus relies on the accelerated radial flow of water into the concrete material under the influence of an externally applied high pressure. The developed FPT method makes use of Darcy's law which relates coefficient of permeability to rate of flow. The apparent coefficient of permeability is computed from the obtained FPT measurements by means of the Packer/Lugeon equation. The flow phenomenon encountered in the FPT was examined from the macroscopic point of view and was based on the continuum approach in which no attention is paid to the pores or the pore structure of the concrete material. The three-dimensional, spherical flow model employed provided the proper analytical solution which constituted the mathematical derivation of the Packer/Lugeon equation presented in this study.

The finalized FPT apparatus consists of two main units namely, the FPT probe which is the actual device inserted into the test hole and which injects pressurized water into the surrounding concrete mass, and the FPT instrumentation unit which provides the central control and the monitoring during a field permeability test run. The developed FPT apparatus is simple and easy to use, and is accompanied by an illustrated user's manual which includes operating instructions and a step-by-step testing procedure.

The FPT apparatus was extensively evaluated by performing the FPTs on numerous bridge structures throughout Florida and also on concrete test

blocks in the laboratory. While the initial moisture content or degree of saturation of the concrete could have a significant effect on the FPT results, consistent results were obtained when the test section was pre-saturated prior to testing. It has been established that test variables such as test orientation, partially filled test section, removal of the probe from the test hole between sequential or repetitive test runs, and level of applied test pressure should not have any significant effect on the final flow measurements obtained during an FPT.

It is believed that the findings from this research study can further be used to compile improved design and construction guidelines and quality/performance requirements for the durability of concrete exposed to marine environments. This study can also provide an effective method for determining the rate of deterioration and, thus, the estimated service life of concrete structures based on in situ and laboratory data. Therefore, a proposed testing scheme which incorporates the developed FPT method was presented.

Based on the experimental findings of the field and laboratory testing programs, the major conclusions of this research study are summarized as follows:

1. The refinement and modification applied to the FPT probe provided a more simplified set-up and dismantling of the apparatus and, thus an improved overall design of the device was achieved.
2. The developed FPT apparatus and method appear promising in providing a suitable measuring system for the rapid and convenient determination of the in situ water permeability of structural concrete.
3. The FPT apparatus can also be effectively used in long-term testing of structural concrete blocks in the laboratory.

4. The relationship between the coefficients of permeability obtained by the FPT and laboratory permeability test methods was highly significant.
5. The results obtained by the FPT and laboratory permeability test methods demonstrated an improved correlation when the tested concrete was fully saturated ( $R^2 = 0.97$ ) as opposed to partially saturated ( $R^2 = 0.96$ ).
6. There seems to be a linear relationship between the charge passed (coulombs) through a concrete material as measured by the Rapid Chloride Permeability test and its corresponding water permeability.
7. A good correlation ( $R^2 = 0.90$ ) was demonstrated between the results obtained by the FPT and the standard Rapid Chloride Permeability (AASHTO T277-83) Test method.
8. The vacuum pre-conditioning and subsequent pre-saturation of the test section prior to testing appeared to be effective in offsetting the effects of moisture content or degree of saturation of concrete on the FPT results.
9. There seems to be a relationship between permeability and durability of concrete, and structure condition. The concrete material which exhibited durability problems also demonstrated high permeability.
10. The deterioration of concrete in the tested bridge structures was primarily due to corrosion of the embedded steel reinforcement which was caused by the intrusion of chloride ions. The high permeability of the in situ concrete material significantly contributed to this effect.

11. A high variation in performance and durability was observed between concrete bridge structures specified to have the same concrete class.
12. The FPT method can provide a relative measurement of permeability which can be used as an indication of the quality and performance characteristics of structural concrete.

### 7.2 Recommendations

The findings drawn from this research study lead to the following recommendations:

1. The concrete to be tested with the FPT apparatus should be sound and without any signs of deterioration such as scaling, cracking, spalling, and corrosion.
2. The concrete surface should be properly cleaned from any surface irregularities or any marine organisms if the selected test location is within the tidal or splash zones.
3. In case the concrete to be tested is relatively dry, a vacuum pre-conditioning and subsequent pre-saturation of the test section should be applied for about 30 minutes prior to actual testing as described in Appendix A. All the recommendations presented in Appendix A should be strictly followed.
4. During an FPT run, in case a drop of the water level in the manometer at the initial application of pressure is registered, measurements should begin after the drop is accounted for and regular flow rates are observed.
5. The constant rate of flow of water (injection rate) established during an FPT run should be used in the calculation of

the coefficient of permeability. If a recorded test measurement (flow rate) which is within the precision of the measuring device remains unchanged for at least a total of 30 minutes, then this would indicate that a relatively constant rate is achieved.

6. Test pressures should be kept to a minimum level possible to produce a measurable flow.
7. The ranges of the relative coefficients of permeability provided in this study were established based on limited data and the given values are not absolute. Therefore, caution should be taken in interpreting these values.
8. The FPT is recommended to be used in conjunction with other standardized tests for the relative measurement of permeability and as an indicator of the performance and durability of in situ concrete.

APPENDIX A  
FIELD PERMEABILITY TEST--USER'S MANUAL

## FIELD PERMEABILITY TEST--USER'S MANUAL

### Definitions:

The term "FPT probe" refers to the actual device that is inserted into the test hole and which injects pressurized water into the concrete. The term "FPT control unit" refers to the Field Permeability Test instrumentation case containing the control valves and pressure gage as shown in Figure A. The term "FPT apparatus" refers to the entire system which includes both the FPT control unit and the probe.

### Recommendations:

In performing an FPT either on laboratory prepared concrete specimens, on concrete sections obtained from the field, or on in situ concrete, it is recommended that de-aerated water be used. In case this is not feasible, the use of distilled water or potable water which is free from any impurities is the best alternative. Sea-water, water which contains chlorides, sulfides or other ions or elements in any concentration should never be used under any circumstances.

Standard pressurized nitrogen gas bottles (cylinders) should be used in providing the required test pressure in an FPT. Test pressures as high as 75% of the allowable tensile strength of concrete could effectively be applied in performing an FPT. In case the tensile strength of concrete to be tested is not known or cannot accurately be estimated, the lowest possible level of pressure which produces a measurable flow shall be applied. In no case should test pressures higher than 750 psi be applied regardless of the tensile strength of the tested concrete.

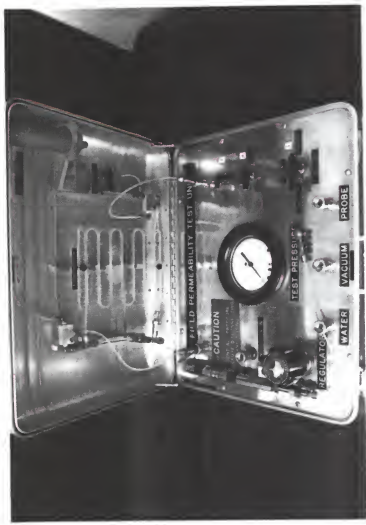


Figure A The Field Permeability Test Instrumentation Case

In case the concrete to be tested is relatively dry, a 30-minute pre-conditioning (pre-saturation) of the test hole should be employed and the moisture content of the in situ concrete should be established before and after an FPT is performed according to the test procedure described in this study.

#### FPT - Operating Procedure

##### Step 1 - Vacuum the System:

- 1.1 Connect the right quick-connect to the control panel on the bottom shell of the FPT control unit (Fig. A1.1).
- 1.2 Turn Reservoir Valve to "REPLENISH" position (Fig. A1.2).
- 1.3 Turn Valve 1 to "VACUUM" position (Fig. A1.3).
- 1.4 Turn Valve 2 to "ON" position (Fig. A1.3).
- 1.5 Turn Valve 3 to alternate position (Fig. A1.3).
- 1.6 Connect the line of the portable hand-operated vacuum pump to the "VACUUM" quick-connect (Fig. A1.3).
- 1.7 Apply full vacuum (30 in.Hg) to the system for approximately 5 minutes (Fig. A1.3), then disconnect the vacuum line from the FPT unit.

##### Step 2 - Introduce Water into the System:

- 2.1 Turn Valve 1 to "WATER" position (Fig. A2.1).
- 2.2 Connect the line of the portable water container to the "WATER" quick-connect (Fig. A2.1).
- 2.3 Wait until the line which is connected to the bottom of the reservoir mounted on the top shell of the FPT unit is filled with water, and then close the reservoir "REPLENISH" Valve.
- 2.4 Wait until the reservoir and all the lines in the system are filled with water, and then disconnect the water line from the FPT unit.

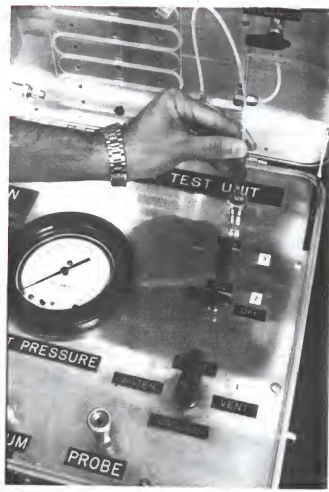


Figure A1.1 FPT - Operating Procedure: Step 1.1

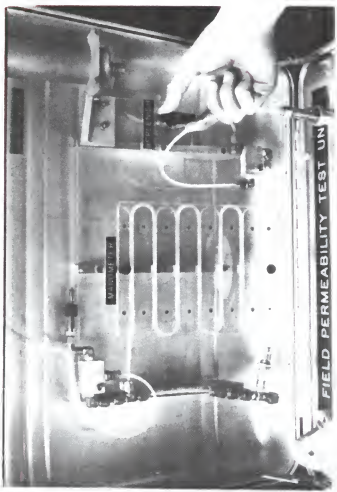


Figure A1.2 FPT - Operating Procedure: Step 1.2

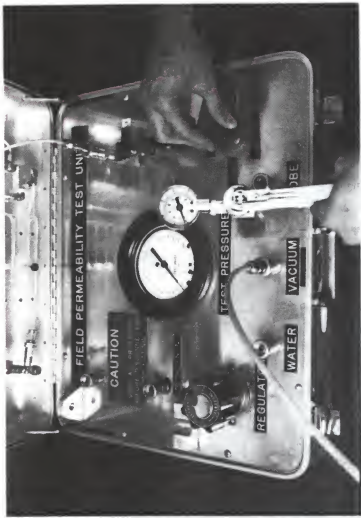


Figure A1.3 FPT - Operating Procedure: Steps 1.3 through 1.7

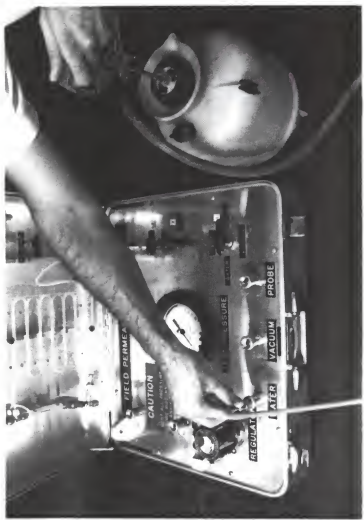


Figure A2.1 FPT - Operating Procedure: Steps 2.1 and 2.2

Step 3 - Set Up the FPT Control Unit for Testing:

- 3.1 Connect the left quick-connect to the control panel on the bottom shell of the instrumentation case - CAUTION: Release any pressure from the system by turning Valve 1 to "VENT" or "VACUUM" position and make sure that the test gauge indicates zero pressure before connecting the lines (Figure A3.1).
- 3.2 Turn Valve 3 to "ON" position (Figure A3.2).
- 3.3 Turn Valve 2 to "OFF" position (Figure A3.2).
- 3.4 Turn Valve 1 to "TEST" position (Figure A3.2).
- 3.5 Connect the pressure source to "NITROGEN IN" on the control panel (Figure A3.2).
- 3.6 Adjust the externally applied pressure to the desired level of test pressure, e.g. 200 psi as indicated by the gauge, by turning the pressure regulator knob clockwise (Figure 3.2).
- 3.7 Open Valve 2 very slowly to let the water level in the test line drop to the manometer level, then turn Valve 2 to the "OFF" position again when the desired level is reached.

Step 4 - Fill Test Hole with Water and Set Up the FPT Probe for Testing:

- 4.1 Connect one end of the test line to the FPT probe (Figure A4.1).
- 4.2 Insert the FPT probe into the test hole, and connect the free end of the test line to the quick-connect of the portable water container (Figure A4.2).
- 4.3 Pressurize the water container to fill the test line and test hole with water. Sustain enough pressure to over-fill until water flows out of the test hole (Figure A4.3).
- 4.4 With the test hole over-filled, start assembling the FPT probe by turning the top nut very slowly clockwise while water still flows



Figure A3.1 FPT - Operating Procedure: Step 3.1



Figure A3.2 FPT - Operating Procedure: Steps 3.2 through 3.6



Figure A4.1 FPT - Operating Procedure: Step 4.1



Figure A4.2 FPT - Operating Procedure: Step 4.2

Figure A4.3 FPT - Operating Procedure: Step 4.3



out of the test hole (Figure A4.4). Continue until the packers are fully expanded and the test hole is securely sealed.

4.5 Disconnect the test line from the water container and connect the free end to the "PROBE" quick-connect on the control panel - CAUTION: Make sure that Valve 1 is at the "VENT" position and Valve 2 is at the "OFF" position (Fig A4.5).

Step 5 - Start Testing:

5.1 Mark the initial position of the water level in the manometer, and set the timer.

5.2 While turning Valve 2 to the "ON" position, start the timer and observe the initial drop of the water level in the manometer (Fig. A5.1).

5.3 Check all the fittings, connections, the test line to the FPT probe, and the test hole for any leakage (Fig. A5.2).

5.4 If, after the initial drop of the water in the manometer is accounted for, no leakage occurs and normal water flow is observed, repeat Step 5.1 and begin test measurements at regular time intervals. A typical time increment of 10 minutes can be used for recording the flow. However, the time increment, can be adjusted depending on the actual flow rate. Readings are continued until a steady-state flow condition is attained.

5.5 When the water has reached the lower level of the manometer tubing, turn Valve 2 to the "OFF" position and stop the timer (Fig. A5.3).

5.6 Turn Reservoir Valve to the "REPLENISH" position and then open the Pressure Relief Valve of the manometer very slowly (Fig. A5.4).

5.7 Let the water refill the manometer to the upper level and then close the Reservoir Valve. Now close the Pressure Relief Valve.



Figure A4.4 FPT - Operating Procedure: Step 4.4

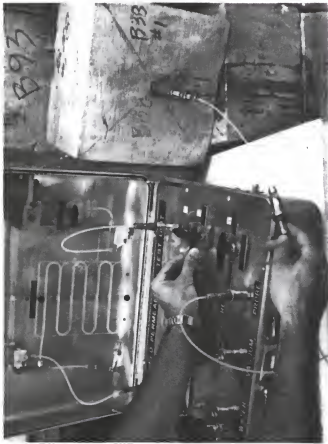


Figure A4.5 FPT - Operating Procedure: Step 4.5

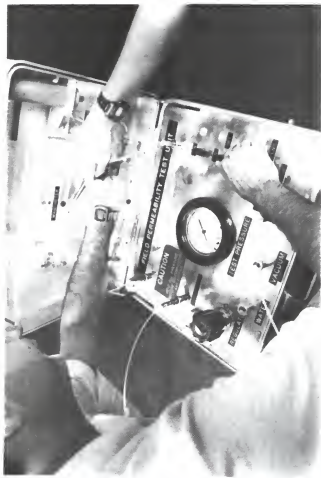


Figure A5.1 FPT - Operating Procedure: Step 5.2



Figure A5.2 FPT - Operating Procedure: Step 5.3



Figure A5.3 FPT - Operating Procedure: Step 5.5



Figure A5.4 FPT - Operating Procedure: Step 5.6

- 5.8 Turn Valve 2 to the "ON" position, start the timer, and resume testing and regular measurements as before.
- 5.9 Repeat Steps 5.5 through 5.8 as many times as necessary to complete the FPT measurements on the tested concrete.

Step 6 - Terminate Testing and Remove FPT Probe from Test Hole:

- 6.1 Turn Valve 2 to the "OFF" position.
- 6.2 Release the externally applied test pressure by turning the regulator knob counter-clockwise; pressure gauge should indicate a zero reading now.
- 6.3 Turn Valve 1 to the "VENT" position.
- 6.4 Open the Pressure Relief Valve and release the pressure in the manometer.
- 6.5 Disconnect the test line from the control panel and from the FPT probe.
- 6.6 Release the packers by turning the top nut of the FPT probe counter-clockwise, and remove the probe from the test hole.

The above FPT run can be conducted by one person plus an assistant, and can be completed within two hours from the commencement of the operation. Under actual field conditions, the entire FPT operation including coring, pre-conditioning, testing, and patching of concrete can be completed within approximately two to three hours.

APPENDIX B  
APPLICATION OF THE PROPOSED TESTING PROGRAM  
FOR MARINE STRUCTURES

### APPLICATION OF THE PROPOSED TESTING PROGRAM FOR MARINE STRUCTURES

The description of the proposed testing program is presented in Chapter 6. The proposed testing scheme can be divided into two major parts namely, the Field Testing Program (A) and the Laboratory Testing Program (B) which subsequently merge into the final evaluation stage (C). This integrated testing scheme is characterized by its efficiency, and ability for vertical and horizontal communication within the program. A number of operations within each part could be performed independently and at a different time while operations between each part could be performed concurrently.

It should be noted that this testing scheme was presented for the sole purpose of demonstrating the potential for future implementation of the developed FPT method in assessing the relative performance and durability of concrete in marine structures. The determination of the applicability, reliability, and effectiveness of all other test methods recommended to be used in conjunction with the FPT in this testing program was beyond the scope of this study. The user could easily modify this program to fit his specific needs, and other test methods judged suitable for the particular purpose of each testing could be incorporated in this program. The implementation of this testing program is not limited to marine concrete structures but it could also be applied to other concrete structures exposed to either similar conditions or to aggressive environments imposing the same deteriorating effects.

Although the assumed data, values, or quantities of the referred parameters are hypothetical in the following example they represent realistic magnitudes for demonstration purposes.

For the worked example presented here it is assumed that the structure under investigation is a 7-year-old concrete bridge with elements of its substructure exposed to ocean waters. This concrete bridge structure was designed for a 75-year service life. The following material data are provided for this structure:

Concrete class = IV

Cement type = II

Aggregate type = porous limestone

Max. aggregate size = 1/2 inch

Water/cement (w/c) ratio = 0.38

Assessment of the Performance and Durability of Concrete in Marine Structures--Worked Example on the Application of the Proposed Testing Program: Refer to the flow chart presented in Figure 6.1.

A. Field Testing Program (refer to Section 5.2).

1. Determination of FPT-INDEX:

Average FPT coefficient value =  $9.55 \times 10^{-9}$  cm/sec

Adjustment factor = (1 / 1.70) = 0.588

K-INDEX =  $(0.588) \times 9.55 \times 10^{-9} = 5.62 \times 10^{-9}$  cm/sec

FPT-INDEX = relative permeability = High (From Table 6.1)

2. Sample Coring:

Refer to Step 5, Section 5.2.1.

3. Electrode Potential Measurements:

Measurements were taken according to the Standard Test Method for Half Potentials of Reinforcing Steel in Concrete, ASTM Designation: C876-87.

Average potential measured = -0.39 V (High)

According to ASTM C876-87, if potentials over an area are more negative than -0.35 V, there is a greater than 90% probability that reinforcing steel corrosion is occurring in that area at the time of measurement.

#### 4. Other Corrosion Data:

- i) Corrosion medication systems, i.e., Cathodic Protection (CP) systems such as impressed current, sacrificial anode, etc. are not installed. In case a CP system was installed, the operation and the effectiveness of the system in providing the required protection to the reinforcing steel had to be evaluated.
- ii) Disbondment of the epoxy coating on reinforcing steel bars at deteriorated sections was observed.
- iii) Extensive vertical cracking at locations within the splash zone of partially submerged concrete piles was observed.
- iv) The concrete cover over reinforcing steel measured at several locations was determined to be less than the required 4-inch cover specified in the design.

#### B. Laboratory Testing Program

##### 1. Determination of the Chloride Ion Concentration in the Sea Water:

The average concentration of the chloride ions in sea water samples obtained from the test location was determined to be 15,500 ppm.

According to the FDOT design guidelines, if the chloride ion concentration is greater than 2,000 ppm the region at which the

concrete bridge under evaluation is situated is classified as an extremely aggressive (highly corrosive) environment.

2. Determination of the Chloride-Ion Permeability (refer to Section 5.3):

Rapid chloride permeability tests were performed according to the Standard AASHTO T277-83 Method on prepared cored concrete samples obtained from the field.

Average total charge passed = 17,500 coulombs (High)

According to AASHTO T277-83, if the total charge passed is greater than 4,000 coulombs the concrete tested is classified to have high chloride permeability, i.e., the concrete material tested is highly permeable to chloride ions. The concrete material tested had a w/c ratio of 0.38. According to AASHTO T277-83, concrete material of low w/c ratio (<0.4) is expected to produce results ranging between 1,000 to 2,000 coulombs which correspond to low chloride permeability.

3. Determination of the Chloride Content in the Concrete Material:

The cored concrete samples extracted from each FPT hole were further analyzed in the laboratory using the Florida Test Method (FM) 5-516 (Determining Low-Levels of Chloride in Concrete and Raw Materials) in order to determine the chloride content of the site concrete material.

Average chloride content at steel depth = 2.9 lbs/cu.yd. of concrete material.

4. Determination of Chloride Intrusion Rate:

Average chloride content at steel depth = 2.9 lbs/cu.yd.

Chloride content to corrosion threshold = 1.20 lbs/cu.yd.

Typical chloride content of new concrete = 0.22 lbs/cu.yd.

Age of bridge structure under investigation = 7 years

Average chloride intrusion in 7 years =  $2.9 - 0.22 = 2.68$  lbs/cu.yd.

Chloride intrusion rate per year =  $2.68 / 7 = 0.383$  lbs/cu.yd./yr

#### 5. Assessment of Corrosion Risk:

##### i) Estimated Time to Corrosion

Chloride intrusion to corrosion threshold =  $1.20 - 0.22 = 0.98$  lbs/cu.yd.

Time to corrosion after construction completion date =  $0.98 / 0.383$  = 2.56 years < 7 years ;

Corrosion Risk = Very High

##### ii) Corrosion State

Based on the electrode potential measurements the corrosion of the embedded reinforcing steel is at an advanced state. Based on all the other corrosion data, the corrosion state can be classified as severe.

#### 6. Laboratory Permeability Tests:

Based on the material information provided for the concrete bridge structure under investigation, an expected permeability range can be assigned for concrete class IV having the specified quality and design. This permeability range can be obtained from the existing permeability data base on Florida concretes (see Reference 31).

Expected permeability range =  $9 \times 10^{-12} -- 6.5 \times 10^{-11}$  cm/sec

In case where 4-inch diameter cored concrete samples could be extracted from the structure, it is suggested that actual long-term laboratory permeability tests be performed on these specimens using

the laboratory permeability test set-up in order to establish a more precise value of the coefficient of permeability of the tested site concrete.

C. Final Evaluation Stage:

At this point the testing program merges to the final evaluation stage where all of the above data are considered.

i) Durability Index

The following durability indices are arbitrarily assigned to reflect the durability characteristics of structural concrete with respect to permeability (water permeability and chloride-ion permeability) of the concrete material tested.

Durability Index

0	=	Not Applicable or Insufficient Data Provided
I	=	Very Poor
II	=	Poor
III	=	Moderate
IV	=	Good
V	=	Very Good
VI	=	Excellent

The tested site concrete material exhibited high permeability as reflected by the FPT-Index and the Chloride-Ion Permeability values obtained in this analysis. The average in situ water permeability coefficient was about 86.5 times higher than the upper limit of the expected permeability range applicable for the concrete material tested. Based on the charge passed (coulombs) through the tested concrete, the chloride permeability was about 8.75 times higher than the upper limit of the expected range applicable for the

concrete material tested ( $w/c = 0.38 < 0.4$ ). Based on the obtained experimental data and the above analysis, a durability index = III (Poor) is thus assigned to the structural concrete material tested.

### ii) Performance Index

The performance indices are arbitrarily assigned to reflect the characteristics of structural concrete in terms of the degree of deterioration under the given exposure conditions, and with respect to the general performance of its intended function. The specified design service life of a structure is a controlling factor in the assignment of the performance index which, in turn, is directly related to durability. It should be noted that a concrete material is considered to be durable if its quality and performance remain acceptable for the design life of the structure. The durability of concrete in a marine environment is only questionable if it deteriorates to a significant extent within the design life of a concrete structure. Since performance and durability are directly related, the performance indices are assigned according to the same code system employed in the durability index classification for uniformity and direct correspondence.

The tested site concrete material exhibited extensive deterioration due to severe corrosion of the reinforcing steel. The high permeability of the concrete material to both water and chloride ions significantly contributed to this effect. The structural concrete is exposed to a highly corrosive environment with excessive chloride concentration. The chloride intrusion rate was such that corrosion of the reinforcing steel was theoretically initiated before the end of the third year of service. The electrode potential measurements suggest that high corrosion activity

is in place. The information obtained from the inspection and evaluation of the deteriorated concrete suggests that the epoxy coating has not effectively provided the necessary protection to the reinforcing steel against corrosive agents such as chloride ions. At the present chloride intrusion rate and in the absence of any other corrosion medication system, it is estimated that within the next 2 years more than 50% of the reinforcing steel of the structural elements of the bridge substructure will be severely damaged due to corrosion.

Based on the above evaluation, a performance index = II (Very Poor) is thus assigned to the structural concrete material tested. The concrete bridge structure considered in this investigation was designed for a service life of 75 years. At the age of 7 years, it has already exhibited severe durability and performance problems. Under the existing exposure conditions and in view of the concrete deterioration which has already been in place, the remaining effective service life (without any major maintenance or rehabilitation) of this marine structure is estimated to be 3 years.

## REFERENCES

1. Mehta, P. K., Concrete, Structures, Properties, and Materials, Prentice-Hall, Inc., Englewood Cliffs, New Jersey 07632, 1986, Chapter 5, pp. 105-169.
2. Mehta, P. K., "Durability of Concrete in Marine Environment--A Review," Performance of Concrete in Marine Environment, SP-65, American Concrete Institute, Detroit, 1980, pp. 1-20.
3. Mehta, P. K., "Durability of Concrete Exposed to Marine Environment--A Fresh Look," Concrete in Marine Environment, SP-109, American Concrete Institute, Detroit, 1988, pp. 1-23.
4. Tyler, I. L. and B. Erlin, "A Proposed Simple Test Method for Determining the Permeability of Concrete," Journal of the PCA Research and Development Laboratories, Vol. 3, No.3, September 1961, pp. 2-7.
5. McMillan, F. R. and Inge Lyse, "Some Permeability Studies of Concrete," Journal of the American Concrete Institute, Vol. 25, December 1929, pp. 100-142.
6. Norton, P. T. and D. H. Pletta, "The Permeability of Gravel Concrete," Journal of the American Concrete Institute, Vol. 27, May 1931, pp. 1093-1131.
7. Ruettgers, A., E. N. Vidal, and S. P. Wing, "An Investigation of the Permeability of Mass Concrete with Particular Reference to Boulder Dam," Journal of the American Concrete Institute, Vol. 31, March-April 1935, pp. 382-416.
8. Von der Meulen, G. J. R. and J. Van Dijk, "A Permeability-Testing Apparatus for Concrete," Magazine of Concrete Research, Vol. 21, No. 67, June 1969, pp. 121-123.
9. Powers, T. C., L. E. Copeland, J. D. Hayes, and H. M. Mann, "Permeability of Portland Cement Paste," Journal of the American Concrete Institute, Vol. 50, November 1954, pp. 285-298.
10. Murata, J., "Studies on the Permeability of Concrete,' RILEM Bulletin (Paris), New Series, No. 29, December 1965, pp. 47-54.
11. Ludirdja, D., R. L. Berger, and J. F. Young, "Simple Method for Measuring Water Permeability of Concrete," ACI Materials Journal, Vol. 86, No. 5, September-October 1989, pp. 433-439.

12. British Standards Institution, "Test for Water Absorption," BS 1881, Part 5, Methods of Testing Hardened Concrete for Other than Strength, Clause 7, London 1970, pp. 35-37.
13. Levitt, M., "The ISAT - A Non-Destructive Test for the Durability of Concrete," British Journal of Non-Destructive Testing, Vol. 13, No. 4, July 1971, pp. 106-112.
14. British Standards Institution, "Test for Determining the Initial Surface Absorption of Concrete," BS 1881, Part 5, Methods of Testing Hardened Concrete for Other than Strength, Clause 6, London 1970, pp. 27-35.
15. Levitt, M., "Durability of Precast Products," Durability of Concrete, A Supplement to the Consulting Engineer, April-May 1971, pp. 25, 27, 29.
16. Levitt, M., "The Permeability and Absorption of Precast Concrete Products," Civil Engineering and Public Works Review, Vol. 55, No. 642, 1960, pp. 88-90.
17. Figg, J. W., "Methods of Measuring the Air and Water Permeability of Concrete," Magazine of Concrete Research, Vol. 25, No. 85, December 1973, pp. 213-219.
18. Cather, R., J. W. Figg, A. F. Marsden, and T. P. O'Brien, Improvements to the Figg Method for Determining the Air Permeability of Concrete, Central Technical Services, Ove Arup Partnership, 13 Fitzroy Street, London, WIP6NQ.
19. Tanahashi, I., S. Ohgishi, H. Ono, and K. Mizutani, "Evaluation of Durability for Concrete in terms of Watertightness by Permeability Coefficient Test Results," SP-100, American Concrete Institute, Detroit, pp. 187-206.
20. Whiting, D., "Rapid Determination of the Chloride Permeability of Concrete," Report No. FHWA/RD-81/119 Federal Highway Administration, Washington, D.C., 1981.
21. Whiting, D., "In Situ Measurement of the Permeability of Concrete to Chloride Ion," In Situ/Nondestructive Testing of Concrete, SP-82, American Concrete Institute, Detroit, 1984, pp. 501-524.
22. Scheidegger, A. E., The Physics of Flow Through Porous Media, Third Edition, University of Toronto Press, Toronto, 1974.
23. Meletiou, C. A., "Design, Development, and Use of a Field Permeability Test (FPT) Apparatus and Nondestructive Method for the Determination of In Situ Permeability of Structural Concrete," Master's Thesis, University of Florida, 1988.
24. Dullien, F. A. L., Porous Media: Fluid Transport and Pore Structure, Academic Press, Inc., New York, 1979.

25. Bazant, Z. P., Mechanics of Geomaterials, Rocks, Concretes, Soils, Center for Concrete and Geomaterials, Northwestern University, Evanston, Illinois, John Wiley & Sons, Ltd., New York, 1985.
26. Harr, M. E., Groundwater and Seepage, McGraw-Hill, Inc., New York, 1962.
27. Greenkorn, R. A., Flow Phenomena in Porous Media: Fundamentals and Applications in Petroleum, Water, and Food Production, Marcel Dekker, Inc., New York, 1983.
28. Neville, A. M., Properties of Concrete, 3rd Edition, Pitman Publishing, London, 1981.
29. Neville, A. M., and J. J. Brooks, Concrete Technology, Longman Scientific & Technical, Harlow, Essex, U.K., 1987.
30. Bouwer, H., Groundwater Hydrology, McGraw-Hill, Inc., New York, 1978.
31. Tia, M., D. Bloomquist, M.C.K. Yang, P. Soongswang, C. A. Meletiou, P. Amornsivilai, E. Dobson, and D. Richardson, "Field and Laboratory Study of Modulus of Rupture and Permeability of Structural Concretes in Florida," Final Report, UF Project 491-450423412, Department of Civil Engineering, University of Florida, Gainesville, Florida, August 1990.
32. Soongswang, P., M. Tia, D. Bloomquist, C. A. Meletiou, and L. Sessions, "An Efficient Test Set-up for Determining the Water-Permeability of Concrete," Transportation Research Record 1204, Transportation Research Board, National Research Council, Washington, DC, 1988, pp. 77-82.

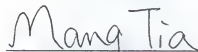
## BIOGRAPHICAL SKETCH

Constantinos A. Meletiou was born April 22, 1960 in Nicosia, Cyprus. In June 1978 he graduated from Acropolis Gymnasium, a Greek secondary school in Nicosia, Cyprus.

He first came to the United States in August 1980 and started undergraduate studies at the University of Florida in the Spring of 1981. He graduated with the degree of Bachelor of Science in Civil Engineering (BSCE) in May 1986. He then returned to his country where he became a registered civil engineer and member of the Council of Civil Engineers and Architects of Cyprus. He was employed for a short period of time as an assistant site engineer at the Cyprus Building and Road Construction Company, Ltd. (CYBARCO). He returned to the University of Florida where he completed the graduate curriculum in construction engineering/civil engineering management, and received the degree of Master of Science in December 1988. He continued graduate studies as a research assistant in the area of concrete materials in pursuit of the degree of Doctor of Philosophy. His current research interests include transport processes in concrete, concrete durability and in situ testing of structural concrete.

Mr. Meletiou is a member of the American Concrete Institute, the American Society of Civil Engineers, the Florida Engineering Society, and an associate member of the Transportation Research Board of the National Research Council.

I certify that I have read this study and that in my opinion it conforms to acceptable standards of scholarly presentation and is fully adequate, in scope and quality, as a dissertation for the degree of Doctor of Philosophy.



Mang Tia, Chairman

Associate Professor of Civil Engineering

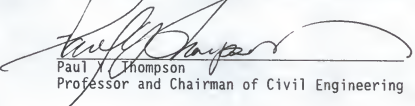
I certify that I have read this study and that in my opinion it conforms to acceptable standards of scholarly presentation and is fully adequate, in scope and quality, as a dissertation for the degree of Doctor of Philosophy.



David Bloomquist, Cochairman

Assistant Professor of Civil Engineering

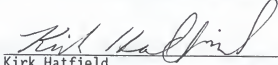
I certify that I have read this study and that in my opinion it conforms to acceptable standards of scholarly presentation and is fully adequate, in scope and quality, as a dissertation for the degree of Doctor of Philosophy.



Paul X. Thompson

Professor and Chairman of Civil Engineering

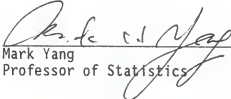
I certify that I have read this study and that in my opinion it conforms to acceptable standards of scholarly presentation and is fully adequate, in scope and quality, as a dissertation for the degree of Doctor of Philosophy.



Kirk Hatfield

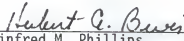
Assistant Professor of Civil Engineering

I certify that I have read this study and that in my opinion it conforms to acceptable standards of scholarly presentation and is fully adequate, in scope and quality, as a dissertation for the degree of Doctor of Philosophy.

  
Mark Yang  
Professor of Statistics

This dissertation was submitted to the Graduate Faculty of the College of Engineering and to the Graduate School and was accepted as partial fulfillment of the requirements for the degree of Doctor of Philosophy.

May 1991

  
for Robert G. Burns  
Winfred M. Phillips  
Dean, College of Engineering

Madelyn M. Lockhart  
Dean, Graduate School